DISSERTATIONES
TECHNOLOGIAE
CIRCUMIECTORUM
UNIVERSITATIS
TARTUENSIS
41

KALEV UIGA

Modelling and experimental measurement of the closed equilibrium systems of $CaS–H_2O$ and $SrS–H_2O$

DISSERTATIONES TECHNOLOGIAE CIRCUMIECTORUM
UNIVERSITATIS TARTUENSIS
41

DISSERTATIONES TECHNOLOGIAE CIRCUMIECTORUM
UNIVERSITATIS TARTUENSIS
41

KALEV UIGA

Modelling and experimental measurement of the closed equilibrium systems of $CaS–H_2O$ and $SrS–H_2O$

UNIVERSITY OF TARTU
Press
1632

Department of Colloid and Environmental Chemistry, Institute of Chemistry, Faculty of Science and Technology, University of Tartu, Tartu, Estonia.

The thesis was accepted for the commencement of the degree of Doctor philosophiae in environmental technology at the University of Tartu on 4. July 2023 by the Scientific Council on Environmental Technology, University of Tartu.

Supervisors: Research Fellow Ivar Zekker, PhD
Institute of Chemistry, University of Tartu, Estonia

Ergo Rikmann, PhD
Institute of Chemistry, University of Tartu, Estonia

Prof. Toomas Tenno, PhD (*In memoriam*)
Institute of Chemistry, University of Tartu, Estonia

Opponent: Prof. Marina Valentukevičienė
Vilnius Gediminas Technical University.

Defence: on 8. Sept, 2023, at 10.15, Chemicum room 1020, 14a Ravila Street, Tartu.

Publication of this thesis is granted by the Institute of Chemistry, University of Tartu, and supported by the following projects: INTERREG research funding of the European Commission “Improving quality of BSR waters by advanced treatment processes”; SLTKT16012 and IUT20-16.

ISSN 1736-3349 (print)
ISBN 978-9916-27-294-7 (print)
ISSN 2806-2612 (pdf)
ISBN 978-9916-27-295-4 (pdf)

University of Tartu Press
www.tyk.ee

In memoriam of Professor Toomas Tenno

TABLE OF CONTENTS

LIST OF PUBLICATIONS INCLUDED IN THE THESIS

This current thesis is based on the following original papers, which are listed below and referred to by their Roman numerals in the text of thesis:

I **Uiga, K.**, Tenno, T., Zekker, I., Tenno, T. Dissolution modeling and potentiometric measurements of the SrS-H_2O-gas system at normal pressure and temperature at salt concentrations of 0.125-2.924 mM. *J. Sulfur Chem.*, 2011 32(2), 137–149; https://doi.org/10.1080/17415993.2011.551937.

II Zekker, I., Tenno, T., Selberg, A., **Uiga, K**. Dissolution Modeling and Experimental Measurement of CaS-H_2O Binary System. *Chin. J. Chem.,* 2011, 29(11), 2327–2336; https://doi.org/10.1002/cjoc.201180399.

III Tenno, T., **Uiga, K**., Mashirin, A., Zekker, I., Rikmann, E. Modeling closed equilibrium systems of H_2O–dissolved CO_2–solid $CaCO_3$. *J. Phys. Chem. A*, 2017, 121(16), 3094–3100; https://doi.org/10.1021/acs.jpca.7b00237.

IV Tenno, T., **Uiga, K**., Mashirin, A., Zekker, I., Rikmann, E., Tenno, T. A novel proton transfer model of the closed equilibrium system H_2O–CO_2–$CaCO_3$–NH_X. *Proc. Est. Acad. Sci*., 2018, 67(3), 260–270; https://doi.org/10.3176/proc.2018.3.04.

V **Uiga, K.**, Tenno, T., Zekker, I., Mashirin, A., Rikmann, E. Modelling and experimental measurement of the closed equilibrium system of H_2O–SrS. *Proc. Est. Acad. Sci.*, 2020, 69(4), 287–297; https://doi.org/10.3176/proc.2020.4.02.

VI **Uiga, K**., Rikmann, E., Zekker, I., Tenno, T. Detection and dissolution of sparingly soluble SrS and CaS particles in aqueous media depending on their size distribution. *Proc. Est. Acad. Sci.*, 2020, 69(4), 323–330; https://doi.org/10.3176/proc.2020.4.07.

Author's contribution

Paper I The author performed all experimental work and data analysis, and was involved in the interpretation of results (on the basis of our developed theoretical model for given systems) and was responsible for the submission of the manuscript as corresponding author.

Paper II The author participated in data collection and was involved in the preparation and submission process of the manuscript (ca 40%).

Paper III The author was one of the initiators of practical studies, participated in data collection and laboratory analyses, writing the manuscript (ca 50%) and was responsible for the interpretation of obtained results and the submission process of the manuscript as co-author.

Paper IV The author was one of the initiators of practical studies, participated in data collection and laboratory analyses (ca 50%) and was responsible for the interpretation of obtained results and the submission process of the manuscript as co-author.

Paper V The author performed all experimental work and partially data analysis and calculations (ca 60%), and was responsible for the interpretation of results as well as the submission process of the manuscript as corresponding author.

Paper VI The author was one of the initiators of practical studies, participated in data collection and laboratory analyses (ca 70%) and was responsible for the interpretation of obtained results and the submission process of the manuscript as corresponding author.

LIST OF ABBREVIATIONS AND ACRONYMS

ACP	average concentration of particles
CFB	circulating fluidised-bed
PF	pulverised firing
K_{SP}	solubility product constant
NTA	nanoparticle tracking analysis
UV-Vis	ultraviolet-visible

DENOTATIONS

$CaS_{(s)}$	solid calcium sulphide
$(H_2S)_w$	dissolved hydrogen sulphide (H_2S) in the aqueous phase
$(H_2S)_g$	dissolved H_2S in gas phase
$[H^+]$	concentration of hydrogen ions (H^+)
$[HS^-]_Z$	concentration of HS^- calculated from charge balance
$[HS^-]_M$	concentration of HS^- calculated from mass balance
f_Z; f_M ($[OH^-]$)	functions of concentrations of protons, calculated from charge balance (f_Z) and mass balance (f_M), respectively
$\Delta[H^+]_{H_2O}$	proton transfers related to water
K_a	the acidity constant of H_2S
K_b	the basicity or the base-dissociation constant of H_2S
K_c	chemical equilibrium constant
K_W	the dissociation constant of the water
pH	a negative logarithm from the concentration of $[H^+]$
S_{total}	sum of concentrations of sulphur species
$SrS_{(s)}$	solid strontium sulphide
ppm	parts per million
t	the temperature in °C

INTRODUCTION

Oil shale industry produces hazardous substances to environment, such as sparingly soluble metal sulphides. Calcium (Ca) and strontium (Sr) are elements collectively known as alkaline-earth metals, which have similar chemical properties. These metals are also represented in various compounds – e.g., with sulphur, they form sulphides, CaS (calcium sulphide) and SrS (strontium sulphide), respectively. These compounds are generated in several industrial processes, including metallurgy and energy production [1,2]. In addition to calcium compounds (e.g., $CaCO_3$, CaO, $Ca(OH)_2$, $CaSO_4$, CaS), traces of Sr (up to 371 $mg \cdot kg^{-1}$, including SrS) have been detected in the oil shale ash processed by the circulating fluidised-bed (CFB) combustion technology in Estonia [3]. Moreover, part of this highly alkaline (pH ≥12) residue (mainly pulverised firing (PF) ash) containing sulphurous compounds (≤2.1%, in mass weight), is used as a fast-acting neutralizer of acidic soils and for the production of building materials. Also, the interaction of VKG's (Viru Keemia Group, AS) semi-coke residue with water (as a result of complex chemical reactions) generates highly alkaline sulphur-rich leachate – a hazardous waste for the environment, which requires further processing or treatment. Besides, part of sulphur from it is emitted into the atmosphere and a toxic gaseous hydrogen sulphide (H_2S_g) is formed [3–14].

Theoretical calculations for determining the exact concentration of formed sulphurous species (e.g., S^{2-}, HS^-, H_2S) are still complicated, mainly due to a large discrepancy of the second acid dissociation constant of H_2S (K_{a2}), ranging from 10^{-12} to 10^{-19} $mol \cdot L^{-1}$ (at temperatures 20–30 °C) [15–20]. A possible explanation for the wide variation of K_{a2} in the published values could lie in the measurement techniques involved (e.g., UV-Vis spectrophotometry, potentiometry (including ion-selective), Raman spectroscopy, etc.). Also, the accuracy of the methods used for determining the concentrations of these formed ions and molecules at equilibrium state affects the calculations [7]. It has been suggested [18] that the use of K_{a2} in calculating the concentrations of sulphur species in aqueous solutions and predicting the solubility of metal sulphides should be avoided because of the uncertainty of the available data in the relevant literature. Moreover, the formed HS^- ions in ambient (sulphur-containing) aqueous solutions, which are also commonly open equilibrium systems, could be oxidized rapidly into sulphates (SO_4^{2-}), sulphites (SO_3^{2-}), thiosulphates ($S_2O_3^{2-}$), and polysulphides (S_n^{2-}) [21–24]. Therefore, in order to avoid the oxidation of these compounds, all measurements should be carried out in the deoxygenated medium by using an inert gas headspace [7–9].

AIMS OF STUDY

The aims of the current PhD thesis were to study the closed equilibrium systems of CaS–H_2O and SrS–H_2O at 25 °C and to upgrade our previously developed mathematical models for these closed equilibrium systems based on the proton transfer principles, which were also experimentally validated. These measured system's pH values were checked in the range of 10.0–13.1. The objectives also included developing non-thermodynamic mathematical models for equilibrium systems containing species of sulphurous compounds. The measurements were taking into consideration all conjugated acid-base processes in order to calculate the pH values, concentrations of formed ions and molecules by using an iteration method [7–9,25].

Besides, the size dependence, the distribution and average concentrations of the formed particles (measured in the range of 10–1500 nm) on the amount of added salt in these systems were studied by using a nanoparticle tracking analysis (NTA). The latter enables to calculate the value of the equilibrium constant (K_c) or the solubility product (K_{SP}) for nanoscale particles in different equilibrium systems and to describe them [25]. More specifically, the aims were:

1) To develop structural schemes and mathematical models for the CaS–H_2O and SrS–H_2O closed equilibrium systems based on the proton-centric principle (where H^+ have the central role by reactions taking place in CaS or SrS aqueous solutions), and to validate them experimentally (**Papers I–VI**);
2) To find out the size dependence and average concentrations of the formed particles (measured in the range of 10–1500 nm) on the amount of added salt in these equilibrium systems. NTA enables to calculate the value of the chemical equilibrium constant (K_c) or the solubility product (K_{SP}) for nanoscale particles (**Paper VI**);
3) To identify the main factors influencing the accuracy of used measurement method (e.g., potentiometry, NTA) for different sulphur species formed in the liquid phase in the CaS–H_2O and SrS–H_2O equilibrium systems (**Papers I–VI**).

1. LITERATURE OVERVIEW

1.1 Origin, nature, production, usage, and solubility of CaS and SrS

1.1.1 CaS and SrS production and usage

Calcium sulphide (CaS) occurs in nature as a mineral oldhamite. Pure CaS is light yellow hygroscopic powder with the odour of H_2S in moist air [1,2,25]. CaS is produced by heating stoichiometric amounts of $CaSO_4$ and carbon (usually as charcoal or coke) under nitrogenous atmosphere at high temperatures (over 850 °C). This process results in the formation of $CaS_{(s)}$ and carbon dioxide $(CO_2)_{(g)}$ as shown in Eq. 1 [26–28]:

$$CaSO_{4(s)} + 2C_{(s)} \rightarrow CaS_{(s)} + 2CO_{2(g).} \quad (1)$$

CaS is an industrially important chemical used in the production of sulphur by the Chance-Claus process, being produced in the treatment of waste liquor from paper mills, it is used as an insecticide and a germicide, as an additive to lubricants and as a flotation agent in ore extraction. CaS is a compound present in luminous paints and varnishes with phosphor. It is also used as a depilatory in leather manufacturing [2]. Beside the technological synthesis of CaS, it is also generated in the retorting process of oil shale contained pyrite and other species of sulphur. More than 50% of the initial sulphur in Estonian oil shale is remained into the solid residue (called as semi-coke) during the retorting process [10–12].

Crude strontium sulphide (SrS) may be obtained by ignition of pulverized strontium sulphate, which occurs in nature as a mineral celestine, with charcoal (also known as the black ash method) up to a temperature of about 1100–1300 ºC, expelling CO_2 from insoluble strontium sulphate to form sparingly water-soluble strontium sulphide (Eq. 2) [2,29,30]:

$$SrSO_{4(S)} + 2C_{(S)} \rightarrow SrS_{(S)} + 2CO_{2(G)}. \quad (2)$$

SrS is used in luminous paints, for dehairing hides, also as a flame retardant in fireworks and for generating H_2S [2].

1.1.2 The solubility of CaS and SrS in water

Calcium and strontium are known as alkaline earth metals in the chemical periodic table (group IIA), thus their chemical properties (including solubility) are similar. Both CaS and SrS have a sodium chloride type of a cubic crystal wire, indicating that the bondages in these salts are highly ionic. They are generally slightly soluble in water, insoluble in alcohols and soluble in acids with decomposition and emission of hydrogen sulphide [1]. Although, CaS and SrS are only slightly soluble in water, their reaction with water causes a significant increase in

the system's pH (while a toxic H_2S forms under anaerobic conditions) that could pose a serious environmental hazard even at small concentrations [1,2,24,25]. Low solubility of CaS and SrS is caused by the strong attraction forces between the ions in the crystal wire, from which they can be separated using the energy released by the solvation process [31]. Thus, the dissolution of solid particles in liquid is dependent on the dissociation and the size of solute molecules [27,32].

The accurate solubility of sparingly soluble salts (including CaS and SrS) is difficult to determine as it also depends on the measuring accuracy of used technique. For the characterization of the behaviour of CaS and SrS in water, it is necessary to know their solubility product (K_{SP}), which value is calculated for less soluble metal salts according to Eq. 3 [1,7,8]:

$$K_{SP} = [M^{2+}]_{(aq)} \times [S^{2-}]_{(aq)}, \tag{3}$$

where $[M^{2+}]_{(aq)}$– metal cation (e.g., $[Ca^{2+}]_{(aq)}$ or $[Sr^{2+}]_{(aq)}$) and $[S^{2-}]_{(aq)}$ (sulphide ion concentration, $mol \cdot L^{-1}$).

Besides, the K_{SP} value is also used for estimating the dissolution rate and the presence of chemical equilibrium of less soluble metal sulphides (e.g. Ag_2S, Hg_2S). However, it is more difficult to accurately calculate K_{SP} value for alkaline earth metal sulphides (e.g. CaS, SrS), because their reaction with water, as released S^{2-} ions binds protons during dissolution, which originate from H_2O. This process is rapid and it lasts until equilibrium state forms in the closed systems of CaS–H_2O or SrS–H_2O [1,27].

Generally, the K_{SP} for metal sulphides are determined from the experimental measurements using the values of the first and second acid dissociation constants (K_{a1} and K_{a2}, respectively) of H_2S. Due to large variation of K_{a2} in the known values, some authors have indicated that its usage in theoretical calculations should be avoided. There has been suggested that more experimental data is needed for better estimation of the accurate value of K_{a2}. There are only few data about the aqueous solubility (or solubility product) of CaS and SrS found in literature, because these slightly soluble (they only partially dissociate into ions in water) hygroscopic salts are stable only in the dry, solid form [7,8,18,29]. Licht (1988) noted that significant amount of free S^{2-} ions in these aqueous solutions of metal sulphides may only exist in concentrated highly alkaline environments, as shown in its hydrolysis equilibrium equation (Eq. 4) [29]:

$$[S^{2-}]_{(S)} + H_2O \leftrightarrow [HS^-]_{(aq)} + [OH^-]_{(aq)}. \tag{4}$$

This very simplified approach (Eq. 4) is not entirely correct, as it assumes a reaction between sulphide ion and water molecule. Actually, the decisive factor in the formation of chemical equilibrium is extremely rapid dissociation of water, where protons and hydroxide ions are released into CaS or SrS aqueous solution. Protons are then taken up and bonded to S^{2-} ions released in the dissociation process of solid CaS or SrS salt, in the closed equilibrium systems of CaS–H_2O

or SrS–H_2O respectively. These processes are carried out according to a novel proton-centric concept (see Figures 1A and 1B) [8,9,29]. Besides, there has been indicated that the alkaline earth metal sulphides are very similar, in their relatively low solubilities, to those shown for their hydroxides. Only some heavier alkali metal salts (e. g., barium) have a substantially higher solubility. Nevertheless, limited and variable values of solubilities (or solubility products, K_{SP}) of the most common alkaline earth metal (Mg, Ca, Sr, Ba) salts (sulphides and hydroxides) in pure water at room temperature and normal pressure are presented in Table 1 [27–30].

Table 1. Known values of solubilities ($g \cdot L^{-1}$) or calculated solubility products (K_{SP}, $mol \cdot L^{-1}$) of the most common (Mg, Ca, Sr, Ba) alkaline earth metal sulphides (MS) and hydroxides ($M(OH)_2$) at room temperature (20 °C [a] or 25 °C [b]) in pure water [27–31].

Content ($g \cdot L^{-1}$)	**Mg**	**Ca**	**Sr**	**Ba**
MS	K_{SP}=**2.0×10^{-18}** $(mol \cdot L^{-1})^2$ [29]	1) **0.212**[a] [28] 2) **1.0**[b] (or K_{SP}=**7.94×10^{-7}** $(mol \cdot L^{-1})^2$ [29])	**10.0**[b] (or K_{SP}=**3.98×10^{-4}** $(mol \cdot L^{-1})^2$ [29])	1) **80.0**[b] [29] 2) **89.4**[b] [27]
$M(OH)_2$	1) **0.0069**[a] [27] 2) K_{SP}=**8.9×10^{-12}** $(mol \cdot L^{-1})^3$ [b] [31]	1) **1.6** [a] [27] 2) **1.0**[b] [29] 3) K_{SP}=**1.3×10^{-6}** $(mol \cdot L^{-1})^3$ [b] [31]	1) **17.4**[a] [30] 2) **10.0**[b] [29] 3) K_{SP}=**3.2×10^{-4}** $(mol \cdot L^{-1})^3$ [b] [31]	1) **47**.0[b] [28] 2) **49.1**[b] [27] 3) K_{SP}=**5.0×10^{-3}** $(mol \cdot L^{-1})^3$ [b] [31]

According to Table 1, possible explanation for a wide variation in measured solubility values of these alkaline earth metal sulphides (MS) and hydroxides ($M(OH)_2$) in literature are mainly due to their low activity coefficient (γ), ion radius (e.g., Ca–99 pm and Sr–113 pm, respectively) and the charge of ions, which influence the reaction rate of certain chemical compound (e.g., the quantity of released S^{2-} ions) in aqueous solution. Besides, the measurement accuracy of used determination method (e.g., UV/Vis spectrophotometry, potentiometry, ion-selective pH measurement, Raman spectroscopy) and a large variation of the K_{a2} (about seven orders of magnitude, ranging from 10^{-12} to 10^{-19} $mol \cdot L^{-1}$ at temperatures 20–30 °C) in the published values are shown, which have been summarized by different researches as seen in Table 2 [17–20,29,32–42].

There has been suggested [18,20] that the use of K_{a2} in calculating the concentrations of sulphur species (e.g., S^{2-}, HS^-, H_2S) in aqueous solutions and predicting solubility of metal sulphides should be avoided because of the uncertainty of the available data in the literature. Besides, formed HS^- ions in ambient aqueous solutions (sulphur-containing open systems) tend to oxidize rapidly into sulphates (SO_4^{2-}), sulphites (SO_3^{2-}), thiosulphates ($S_2O_3^{2-}$) and polysulphides (S_n^{2-}). [18,20,21,23]. Thus, in order to avoid oxidation of CaS or SrS and hydrogen sulphide emissions into the atmosphere, all measurements must be carried out in

the deoxygenated medium by using an inert gas (e.g., argon or nitrogen) closed headspace [7–9,18].

Table 2. Known values of pK_{a2} (negative logarithm of the second acid dissociation constant of H_2S, K_{a2}) with applied determination techniques given in the literature (at temperatures 20–30 °C) [17–20,33–43].

pK_{a2}	Method	Reference(s)
19	Mathematical extrapolation	[33]
17.6±0.3	Ion-selective pH-measurement	[34]
17.4	Sulphidation of sulphur	[20]
17.1±0.2	UV/VIS abs. spectrophotometry	[35]
17	Raman spectroscopy	[36]
16	Densometric analysis	[19]
15.3	Solubility	[37]
15.19	Vapor–liquid equilibrium	[38]
14.92	Solubility	[39]
13.86	Ion-selective pH-measurement	[40]
13.85	UV/VIS spectrophotometry	[41]
13.78	Potentiometry	[42]
12.85	Solubility	[43]
12	Potentiometry	[17]

Earlier studies also indicated that mainly HS^- ions (≥99% of total sulphur species) were presented at measured ranges of pHs (between 9–11) in the closed equilibrium systems of CaS–H_2O or SrS–H_2O, HS^- will be formed after dissociation of these salts in deoxygenated water [7–9,44–47]. In cases like this, where experimental difficulties prevent reliable data being obtained, scientists commonly turn to indirect methods (e.g., extrapolation) in which the properties of the species of interest are predicted by determining the properties of their chemical homologues [20].

According to [48], the aqueous solubility of less soluble compounds in equilibrium with the solid phase is constant and it corresponds to the value of K_{SP} when no chemical reaction takes place in the water phase. The solubility product of molar concentrations of the ions formed in the dissolution has an infinite number of possible values, depending on the conditions, such as the presence of a common ion and the temperature. Thus, chemical precipitation occurs when the concentration of ions in the aqueous phase exceeds the solubility of salt, which is commonly known as supersaturation. The latter is an important concept in order to predict the dissolution rate and precipitation of sparingly soluble salts (including CaS and SrS) in water [8,48,49].

2. MATERIALS AND METHODS

2.1 Derivation of the theoretical models of the closed equilibrium systems of CaS–H_2O and SrS–H_2O

The theoretical models of CaS–H_2O and SrS–H_2O are based on the novel proton transfer conception, which is different from commonly used ones based on thermodynamics [8,9,50–52]. In order to model these self-regulating complex systems, it must be taken to account that the chemical reactions in aqueous solutions will proceed relatively fast compared to other liquids. For example, the dissociation reaction of water into H^+ and OH^- ions is the fastest reaction rate known in the aqueous solutions with rate constant $k = 1.4\times10^{11}\ L\cdot mol^{-1}\cdot s^{-1}$ [48]. The structural scheme of the closed equilibrium systems CaS–H_2O and SrS–H_2O is presented in Figures 1A and 1B. Besides, the formation of gaseous dihydrogen sulphide is not included in the proposed models [7–9].

According to Figures 1A and 1B, Ca^{2+} or Sr^{2+} (both will be further denoted as M^{2+} in equations) and S^{2-} ions are released by the reversible dissolution of CaS or SrS, when a surplus amount of salt is added. At the next step of reaction, the S^{2-} ions will accept a certain number of protons, which originate from the reversible dissociation reactions of water.

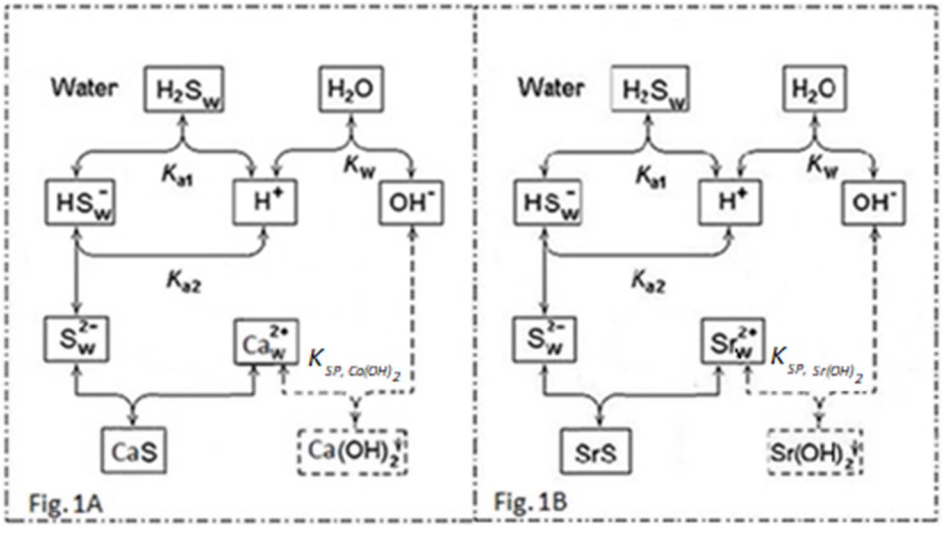

Figures 1A and 1B. Structural scheme of distribution of ions and molecules in the closed equilibrium systems of CaS–H_2O and SrS–H_2O, where: K_{a1} – the first acid dissociation constant of H_2S; K_{a2} – the second acid dissociation constant of H_2S; K_W – the ion-product constant of water; $K_{SP,Ca(OH)_2}$; $K_{SP,Sr(OH)_2}$– the solubility product constants of $Ca(OH)_2$ or $Sr(OH)_2$ [7–9].

Previous studies have indicated that the measured [HS^-] ions in the CaS or SrS aqueous solutions could be underestimated, because part of them might form highly soluble, but very unstable (they probably exist only near room temperature and at certain system's pH values) metal hydrosulphide complexes (e.g., $Ca(HS)_2$ or $Sr(HS)_2$) or ligands with dissociated Ca^{2+} or Sr^{2+} ions. They are formed in the presence of hydrogen sulphide in these equilibrium systems (after dissolution of corresponding salts in purified water) [7,20,21,24,53]. The K_{SP} value of $Ca(OH)_2$ or $Sr(OH)_2$ will be exceeded when surplus amount of CaS or SrS is added into the initial closed equilibrium systems of CaS–H_2O or SrS–H_2O, which contains six different species of ions and molecules in the water phase, namely M^{2+} (Ca^{2+} or Sr^{2+} cations), S^{2-}, HS^-, H_2S, OH^- and H^+. Besides, the precipitates of above-mentioned salts (e.g., CaS, SrS, $Ca(OH)_2$ and $Sr(OH)_2$) will also occur after addition of sodium hydroxide (NaOH) into these equilibrium systems, because it dissolves better and will rise quickly aqueous solution's pH level as more hydroxide ions are formed in aqueous solution [9,52]. These formed ions and molecules are quantitatively distributed in CaS or SrS aqueous solutions in accordance with their equilibrium constants (including $Ca(OH)_2$ or $Sr(OH)_2$, which form at higher [CaS] or [SrS]). Their values are the following (Eqs. 5–11) [7–9,17,29,31,39,54]:

$$K_{a1} = \frac{[H^+]\times[HS^-]}{[H_2S^-]_w} \cong 1.047\times10^{-7}\ \text{mol}\cdot\text{L}^{-1}\ [17], \tag{5}$$

$$K_{a2} = \frac{[H^+]\times[S^{2-}]}{[HS^-]_w} \cong 1.202\times10^{-15}\ \text{mol}\cdot\text{L}^{-1}\ [39], \tag{6}$$

$$K_w = [H^+]\times[OH^-] \cong 1.01\times10^{-14}\ (\text{mol}\cdot\text{L}^{-1})^2\ [54], \tag{7}$$

$$K_{c,SrS} = \frac{[Sr^{2+}]\times[HS^-]}{[SrS]} \cong 1.333\times10^{-3}\ \text{mol}\cdot\text{L}^{-1}\ [7], \tag{8}$$

$$K_{SP,Sr(OH)_2} = [Sr^{2+}]\times[OH^-]^2 = 3.2\times10^{-4}\ (\text{mol}\cdot\text{L}^{-1})^3\ [31], \tag{9}$$

$$K_{c,CaS} = \frac{[Ca^{2+}]\times[HS^-]}{[CaS]} = 1.682\times10^{-3}\ \text{mol}\cdot\text{L}^{-1}\ [29], \tag{10}$$

$$K_{SP,Ca(OH)_2} = [Ca^{2+}]\times[OH^-]^2 = 1.3\times10^{-6}\ (\text{mol}\cdot\text{L}^{-1})^3\ [31]. \tag{11}$$

In order to calculate the closed equilibrium system's pH, concentrations of formed ions and molecules, available values of K_{a1} [17] and different previously published values of K_{a2} [7–9,18] were used. Known values of the K_{a2} in the literature were compared with the experimentally obtained results in the solid [CaS] or [SrS] (range of 0.125–83.552 mM). As a result, the closest correlation between the calculated (different pK_{a2} values were used from 12 to 15) and the measured values of parameters of the investigated systems (CaS–H_2O or SrS–H_2O) was at $K_{a2}=1.202\cdot10^{-15}$ mol·L^{-1} given by Knox et. al (1906) [7–9,39]. Besides, for calculating the concentrations of unknown variables, the base-dissociation or ionization constants (K_{b1} and K_{b2}) are expressed as follows (Eqs. 12–13) [7–9]:

$$K_{b1} = \frac{[H_2S]_W \times [OH^-]}{[HS^-]} = \frac{K_W}{K_{a1}} \cong 9.65 \times 10^{-8}\,\text{mol}\cdot\text{L}^{-1}, \quad (12)$$

$$K_{b2} = \frac{[HS^-][OH^-]}{[S^{2-}]} = \frac{K_W}{K_{a2}} \cong 8.40\ \text{mol}\cdot\text{L}^{-1}. \quad (13)$$

In order to simplify these expressions for the closed equilibrium systems of CaS– H_2O or SrS–H_2O, the charge balance equation (Eq. 14) in the liquid phase is [7–9]:

$$2([M^{2+}]_Z)+[H^+]=2[S^{2-}]+[HS^-]+[OH^-], \quad (14)$$

and the molar balance equation (Eq. 15) in order to calculate the mass of sulphur species in CaS or SrS aqueous solutions is [7–9]:

$$([M^{2+}]_M)=[S^{2-}]+[HS^-]+[H_2S]_w. \quad (15)$$

The concentrations of unknown variables ($[S^{2-}]$, $[H_2S]_w$, $[H^+]$) in charge (Eq. 14) and molar balance (Eq. 15) equations of sulphur species in investigated systems were eliminated by replacing their concentrations from the Eqs. 5–11 with known (experimentally measured) values of $[HS^-]$ and $[OH^-]$ as follows (Eqs. 16–18) [7–9]:

$$[H^+] = \frac{K_W}{[OH^-]}, \quad (16)$$

$$[S^{2-}] = \frac{[HS^-] \times [OH^-]}{K_{b2}}, \quad (17)$$

$$[H_2S]_W = \frac{K_{b1} \times [HS^-]}{[OH^-]}. \quad (18)$$

Besides, the concentration of hydrogen ions can be also found by using the measured pH value of investigated system ($[H^+]=10^{-pH}$). As a result of replacing the variables, these equilibrium systems are characterized by two equations with two unknown concentrations ($[S^{2-}]$ and $[H_2S]_w$). These quite complicated systems should be simplified by elimination of parameters, which are not substantial from the point of view of the accuracy at measured system´s pH ranges of 7–13 (e.g. $[S^{2-}]$). The equilibrium distribution of sulphide forms and the corresponding value of ions' concentration in the liquid phase should simultaneously satisfy the conditions of molar and charge balances in the closed systems of CaS–H_2O or SrS–H_2O. In order to calculate their values by an iterative method, the charge ($[HS^-]_Z$) and molar ($[HS^-]_M$) balance equations were converted to the following forms (Eqs. 19–21) [7–9]:

$$[HS^-] = [HS^-]_Z = f_Z([OH^-]) = \frac{2([M^{2+}]_Z) + \frac{K_W}{[OH^-]} - [OH^-]}{\frac{2[OH^-]}{K_{b2}} + 1}, \quad (19)$$

$$[HS^-] = [HS^-]_M = f_M([OH^-]) = \frac{([M^{2+}]_M) - [H_2S]_W}{\frac{[OH^-]}{K_{b2}} + 1 + \frac{K_{b1}}{[OH^-]}}, \quad (20)$$

$$\Delta[HS^-] = [HS^-]_M - [HS^-]_Z \rightarrow 0. \quad (21)$$

Iterative methods are mainly based on the termination criterion, which allows to eliminate the unknown concentration of formed ions and molecules (when their corresponding values are relatively small) in order to simplify further mathematical calculations in given equilibrium systems. After elimination of the variables that do not have a significant influence on the accuracy of the results, these equations (Eqs. 19,20) contain only one unknown ($[OH^-]$). The latter will be derived from the corresponding pHs of the closed equilibrium systems of CaS–H_2O or SrS–H_2O by using its different values of concentration or will be calculated according to the square root equation (Eq. 22) as follows [8,9]:

$$[OH^-] \cong \frac{[M^{2+}] - K_{b1}}{2} + \sqrt{\left(\frac{[M^{2+}] - K_{b1}}{2}\right)^2 + 2 \times [M^{2+}] \times K_{b1}}. \quad (22)$$

After substitution of the numerical values into the equation, it is possible to calculate the $[OH^-]$ and further find the pHs and corresponding values of the ions (e.g., $[S^{2-}]$, $[HS^-]$) and molecules ($[H_2S]_w$) in the closed equilibrium systems of CaS–H_2O or SrS–H_2O [8,9]. Thus, the solubility of these salts (CaS or SrS) and the rapid dissociation of water will determine the equilibrium of the system. Water acts as a proton donor (the value of K_W must remain constant), because protons will be bound to sulphide (S^{2-}) ions and after that reaction, bisulphide (HS^-) ions will be formed in these equilibrium systems according to a novel proton-centric concept [8,9,50–52,56].

2.2 Nanoparticles – their properties, application and importance by the dissolution of solid SrS or CaS

2.2.1 Properties, importance and application of CaS and SrS nanoparticles

Nanotechnology is a known field of research since last century. It mainly focuses on small particles called nanoparticles (NPs), which have size in the range of 1 to 100 nm. They can be classified into different classes based on their properties, shapes or sizes (besides NPs, also for nanotubes, nanomembranes etc.). The different groups include fullerenes, metal NPs, ceramic NPs, and polymeric NPs. These NPs possess unique physical and chemical properties due to their high surface area and nanoscale size. Their optical properties are reported to be dependent on the size, which imparts different colours due to absorption in the visible region. Their reactivity, toughness (the ability of a material to absorb energy and plastically deform without fracturing) and other properties are also dependent on their unique size, shape and structure.

Due to these characteristics, they are suitable candidates for various commercial and domestic applications, which include catalysis, imaging, medical and environmental ones [57]. For example, sulphide-based luminescent nanomaterials (including CaS and SrS) have attracted a lot of attention for a wide range of photo-, cathodo- and electroluminescent applications (e.g., flat panel displays based on thin film electroluminescence, field emission displays). This is mainly due to their ability (in contrast to oxide materials) to provide a broad band (over the entire visible region 380–760 nm) by appropriately choosing the composition of the sulphide host [58,59]. Besides, Wu et. al (2011) have found that the developed Fe–CaS NPs have a great potential in cancer treatment as a medical cure method [60]. Heavy metal NPs of lead, mercury and tin are reported to be so rigid and stable that their degradation is not easily achievable, which can lead to toxic effects, because of their small size and ability to penetrate the membranes of cells [57]. Thus, the dissolution rate of NPs in aqueous solutions of alkaline-earth metal salts is an important parameter by determining their safety as it strongly affects the uptake pathway, toxicity, and the extent of potential environmental impact [57,61–67].

2.2.2 Theoretical background of the dissolution mechanism of SrS or CaS particles (including NPs)

Previous studies have shown that the abundance of NPs in the closed equilibrium systems (including CaS–H_2O and SrS–H_2O) results in a faster increase of the system's pH values due to NPs larger specific surface area when solid CaS or SrS is added into MilliQ water [7–9,25,62].

As described in paper IV, after dissolution of solid CaS or SrS, formed particles (including NPs) are surrounded by an aqueous medium as their solvation

(or hydration when the solvent is water) and dissociation into ions takes place in the liquid phase [8,9,25]. Additional energy by elevating system's temperature is required to overcome the intermolecular interactions (e. g. van der Waals and electrostatic forces) that occur in a solute. The unequal charge distribution in polar liquids such as water, where the bonds between molecules in a liquid are constantly breaking and reforming, makes them good solvents for ionic compounds, including sparingly soluble CaS and SrS. As a result of their hydration process in aqueous media, the oxygen atoms of the H_2O molecules surround the cations (Ca^{2+} or Sr^{2+}) and the hydrogen atoms (protons) react with the released anions (S^{2-}) [25,62,68].

Besides, the pH of CaS or SrS aqueous solutions is a key parameter in evaluating the interactions between formed ions and molecules in these equilibrium systems. In order to provide a larger electrostatic interaction with the water molecules, they must be oppositely charged. Thus, the lower absorption in the acidic solutions is attributed to the protons competing with the metal ions for exchange sites [25,62,69].

Theoretical explanations about dissolution processes are so far mainly based on thermodynamics, which do not take to account the interaction between the particles of the solvent and the soluble matter, as well as the inter-particle interactions occurring within the phases of each environment and their interface area. In the case of a smaller diameter of the solid-phase particles, the curvature of their surface is larger, and thus, the particles on the surface are weakly bound to the ones in the inner and side layers of the solid phase and can be more easily transferred from the solid to the liquid phase. By dissolution of salts and dissociation of water these processes are affected by ionic radius and many intermolecular forces, including the hydrogen bonding, the dipole-dipole interactions, and the Van der Waals forces. Chemical reactions occurring in the liquid phase will lead to a new equilibrium to be established in this phase, and thereby, will also change the existing balance on the boundary surface of the solid-liquid phase. Thus, the generally accepted concept is that neither the amount of excess solid nor the size of the particles present in the system will change the position of the equilibrium [25, 62, 68–70].

2.3 Used materials and methods for analysing the samples from deoxygenated CaS or SrS aqueous solutions

2.3.1 Experimental materials and procedures for the determination of CaS or SrS salt solubility and pH

The solubility of CaS or SrS salt was determined potentiometrically by using a pH-meter, after which the ratios of the measured and theoretical concentrations of dissolved ions and molecules (Ca^{2+} or Sr^{2+}, OH^-, H^+, HS^-, H_2S, and S^{2-}) were compared in the CaS–H_2O or SrS–H_2O equilibrium systems. For experimental measurements, only analytical grade reagents (with purity of 99.9%, provided by

Alfa Aesar, Germany) were used and the determinations of ions from CaS or SrS aqueous solutions were performed after reaching to the equilibrium state, which could be seen by the stabilization of the measured system's pH value. Each determination was made in at least three replicates in order to achieve a sufficient confidence level.

Solid CaS or SrS were weighed with analytical balance (Scaltec SBC 31, Germany; measuring accuracy of ±0.001 g) just before their addition into the MilliQ water (1000 mL), which was also purged with argon (99.999% Ar) or nitrogen (99.9% N_2) for about half an hour before salt addition in order to remove oxygen (O_2) and carbon dioxide (CO_2). The latter is needed to avoid the oxidation of sulphide (mainly HS^-) ions and the precipitation of calcium or strontium carbonate. The efficiency of oxygen removal was controlled by the measurements of dissolved oxygen (DO) in water (oxygen-meter Marvet Junior MJ2000, Elke Sensor, Estonia).

The experiments were carried out at normal pressure (101325 Pa) in air-tightly closed glass bottles (with the volume of 1200 mL), which were filled with purged (argon or nitrogen) MilliQ water and inserted into a thermostated water bath (Hecht-Assistent Magnetmix 2070 or Assistent 3180, Germany) with a magnetic stirrer (Stuart Scientific magnetic stirrer SM5) in order to keep a constant temperature of 25±0.2 °C and a stirring speed of about 150–200 revolutions per minute (rpm) during measurements.

The pH's of the prepared CaS or SrS aqueous solutions were measured potentiometrically in at least three replicates by using the pH-meter (Jenway 3520, UK), which was connected to a special pH-electrode (Jenway model No. 924-076, standard error of ±0.003) intended for highly alkaline solutions. The latter was calibrated before each measurement at pH values of 7.00, 10.00, and 13.00 in buffer solutions with a standard error of ±0.002. The pH electrode was inserted tightly into the cover of the reaction cell, which was connected with a computer and a program for measurement (Dataway version 1.1; Jenway, UK), registering the corresponding pH values of CaS or SrS aqueous solutions. Statistical significance (p-value) of measured results was calculated by MS Excel 2003 program [7–9, 25].

The total amount of sulphur-containing species (the sum of dissolved H_2S, HS^- and S^{2-}) was determined iodometrically, where the excess of added iodine was titrated back with sodium thiosulphate [71,72]. Typically, a sample of 5–20 mL was collected for analysis and acidified below pH=10 with 0.1 M HCl. For comparison with titration, the concentration of bisulphide was measured by UV-Vis spectrophotometry, where the received calibration curve was linear within the studied range ($[HS^-]$=1–9 $mg \cdot L^{-1}$) [7–9,25,73–76]. A scanning UV-Vis spectrophotometer (Perkin Elmer, Lambda 35, UK) with a 10-mm quartz cell was used for absorbance measurements of the $[HS^-]$ ions in the CaS or SrS aqueous solutions against MilliQ water as a blank. The characteristic peak of bisulphide (HS^-) ion appears clearly on the UV spectra (at 231 nm), and the intensity of the UV band is related to its concentration in measured sample [74,76].

The $[HS^-]$ ions in the sample were determined by the calibration curve, prepared through preliminary measurements by using sodium bisulphide (99.9%,

Alfa Aesar, Germany). The time for the analysis after the dissolution process was considered to be critical because of a possible oxidation of samples which could get in contact with air [29,75,77,78]. To avoid this, all analyses were carried out immediately after reaching the equilibrium state in the CaS or SrS aqueous solutions and the collected samples were kept in closed cuvettes under inert gas (argon) [7–9,25]. The concentration of calcium or strontium ions (only these alkaline-earth metal ions were present in measured aqueous CaS or SrS solutions) was determined by direct titration with ethylene-diamine tetraacetate (EDTA) [7–9,71].

2.3.2 Determination of hydrosulphide bonding rate from SrS aqueous solution in a closed test system

A closed SrS–H_2O test system (without oxygen access) was used to determine the average bonding rate of gaseous hydrosulphide $(H_2S)_g$ by an alkaline (NaOH) solution. Air-tight closed glass bottles with a volume of 1.0 litre were used for measurements. In this system, 50 mL of 0.5 M NaOH solution (pH∼13.7) was used for capturing hydrosulphide from the gas phase of the reaction cell.

For the preparation of 4.18–16.71 mM SrS aqueous solutions (volume of 200 mL), deoxygenated MilliQ ultrapure water was used to avoid the oxidation of sulphide ions during the experiments. In the closed test system, oxygen was removed with argon (Ar) gas from the gas phase of the reaction cell. All the experiments were carried out at a constant temperature (25±1 °C) and at a normal pressure. A magnetic stirrer (Hecht-Assistent Magnetmix 2070, Germany) was used (at a constant stirring speed of 400 rpm) for mixing the prepared SrS solutions. The experiments in the closed reaction cell (Figure 2) lasted for 68–238 h [7].

Figure 2. Closed test system with the SrS aqueous solution.

At the end of the experiments, the glass bottles were opened and the samples were collected for analysis, which were made immediately. The concentration of the dissolved sulphide ions was determined in 0.5 M NaOH solution by iodometric titration and the [Sr^{2+}] ions by titration with EDTA. Besides, the pH of these SrS aqueous solutions were also measured (Jenway 3510, UK) and obtained results were registered with a program for measurement (Dataway version 1.1; Jenway, UK) (**Papers I–VI**) [7–9, 50–52].

2.4 The detection and characterization of NPs in CaS or SrS aqueous solutions by using Nanoparticle Tracking Analysis (NTA)

NTA is the most common technique used for detection and for describing the nanoscale particles in different solutions. It provides direct and real-time visualization, sizing, and counting of particulate materials in size between 10–2000 nm in liquid suspension using only a metallized optical element illuminated by laser beam, a conventional optical microscope fitted with an inexpensive camera and dedicated analytical software. This technique works on a particle-by-particle basis, relating the degree of movement under Brownian motion to the sphere equivalent hydrodynamic diameter particle size, allowing high resolution particle size distributions and counting to be obtained within few minutes. The instrument generally records a video of the moving particles at a given frame rate, which allows for the determination of the location of all the particles in the observation area for each recorded frame. This allows the software to construct dynamic model for the observed particles, including their movement tracks and number of steps, which will take them to cover the distance. The computer program analyses each frame of the video determining the location of the observed particles by using a modified Stokes–Einstein equation (Eq. 22) to calculate the hydrodynamic diameters of each individual one, as follows [79–85]:

$$\underline{(x,y)^2} = \frac{2k_B T}{3r_h \pi \eta} \quad [83], \tag{22}$$

where k_B is the Boltzmann constant and $\underline{(x,y)^2}$ is the mean squared speed of a particle at a temperature T (in Kelvin degrees), in a medium of viscosity (η), with a hydrodynamic radius of r_h.

Previous studies have shown that this technique is very accurate for sizing both monodisperse and polydisperse samples, because it has a substantially better peak resolution compared to other similar methods. Besides, NTA allows the measurement of large amounts of particles, compared to transmission electron microscopy (TEM), and it has been applied to a wide range of materials including metals, metal oxides and polymers [62,79,83–87].

In order to count and measure the particles sizes in aqueous media, their detection and tracking analysis was carried out by applying standard measurements of a NanoSight LM10 Viewing Unit (Malvern Instruments Ltd., United Kingdom). Measurements were made at a controlled temperature of 25 °C by using a cuvette, where prepared samples of known concentrations of deoxygenated CaS and SrS aqueous solutions were carefully injected in order to avoid the formation of nanobubbles, which may affect the obtained results. For each measurement, prepared samples were injected 5 times with three repetitions in order to receive results with a sufficient confidence level [25,79].

3. RESULTS AND DISCUSSION

3.1 The results of theoretical calculations and experimental measurements of CaS–H_2O or SrS–H_2O closed equilibrium systems

Experimental study was conducted with the purpose of controlling the validity of the developed theoretical models of CaS–H_2O and SrS–H_2O. The results of the experimental measurements of these closed equilibrium systems indicated that the concentration values of formed ions (e.g., $[Ca^{2+}]$, $[Sr^{2+}]$, $[OH^-]$, $[H^+]$, $[HS^-]$) in measured CaS and SrS aqueous solutions were close to the theoretically calculated ones, as seen in Tables 3, 4A and 4B. The calculations of the final closed equilibrium system's concentrations of formed ions and molecules ($[Ca^{2+}]$ or $[Sr^{2+}]$, $[S^{2-}]$, $[H_2S]_w$), and the corresponding systems' pHs were performed on the basis of the calculated concentrations of $[HS^-]$ and $[OH^-]$ or $[H^+]$ ions at equilibrium state. Furthermore, the quantity of protons bound by S^{2-} ions and the quantity released from the dissociation of water ($[H^+_{H_2O}]$) were also taken into consideration [7–9,50–52]. In order to calculate the closed equilibrium systems' pHs, concentrations of formed ions and molecules, different previously published values [7,18] of K_{a2} were compared with the experimentally obtained results in the range of [CaS] 0.335–1.823 mM and [SrS] 0.125–83.552 mM, respectively [7–9]. As a result, the closest correlation between the calculated and the measured values of parameters of the investigated closed equilibrium system CaS–H_2O or SrS–H_2O systems was at $K_{a2}=1.202\cdot10^{-15}$ mol·L^{-1} (Figure 3) and the results are shown in Tables 3, 4A and 4B [7–9,39].

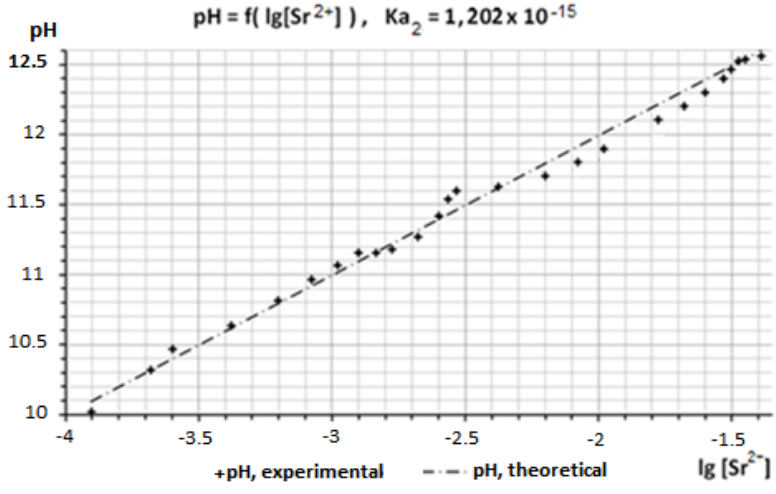

Figure 3. Correlation between measured and theoretically calculated ($K_{a2}=1.202\cdot10^{-15}$ mol·L^{-1}) pH values of the SrS–H_2O closed equilibrium system at concentration of $[Sr^{2+}]$ ions from 0.125 to 41.776 mM [9].

Table 3. Amounts of added CaS into 1 L of purified water and measured concentrations of $[Ca^{2+}]$, $[OH^-]$ and $[S_{total}]$ [8].

$[CaS]_S$, mM (SD ±)	$[Ca^{2+}]$, mM (SD ±)	$[OH^-]$, mM (SD ±)	$[S_{total}]$, mM (SD ±)	pH (SD ±)
0.335 (±0.020)	nd	0.398 (±0.019)	0.325 (±0.06)	10.60 (±0.02)
0.554 (±0.049)	nd	0.679 (±0.049)	0.546 (±0.02)	10.83 (±0.03)
0.832 (±0.010)	0.825 (±0.010)	0.918 (±0.021)	0.783 (±0.07)	10.96 (±0.01)
1.123 (±0.010)	1.112 (±0.003)	1.358 (±0.097)	1.100 (±0.02)	11.13 (±0.03)
1.375 (±0.004)	1.378 (±0.020)	1.479 (±0.106)	1.360 (±0.02)	11.17 (±0.03)
1.386 (±0.094)	1.384 (±0.010)	1.486 (±0.143)	1.372 (±0.05)	11.17 (±0.04)
1.516 (±0.020)	1.490 (±0.008)	1.679 (±0.079)	1.487 (±0.05)	11.22 (±0.02)
1.650 (±0.013)	1.652 (±0.010)	1.778 (±0.012)	1.587 (±0.10)	11.25 (±0.01)
1.733 (±0.006)	**1.719 (±0.006)**	**1.820 (±0.047)**	**1.696 (±0.05)**	**11.26 (±0.01)**
1.774 (±0.010)	1.744 (±0.060)	1.950 (±0.097)	1.740 (±0.05)	11.29 (±0.02)
1.823 (±0.010)	1.795 (±0.006)	2.061 (±0.068)	1.760 (±0.05)	11.31 (±0.01)

nd – not determined

Table 4A. Calculated concentration of formed ions, molecules and pH in the equilibrium system of SrS–H_2O (0.125–83.552 mM), where K_{a1}=1.047·10^{-7} mol·L^{-1} [17]; K_{a2}=1.202·10^{-15} mol·L^{-1} [31] and K_W=1.01·10^{-14} (mol·L^{-1})^2 at 25 ºC [7,9].

$[SrS]_S$ mg·L^{-1}	$[Sr^{2+}]$ mM	$[S^{2-}]$ mM, %	$[HS^-]$ mM, %	$[H_2S]_w$ mM	$[OH^-]$ mM	pH (calc.)
15	0.125	4.0×10^{-6} (0.003%)	0.1249 (99.920%)	9.68×10^{-5} (0.077%)	0.123	10.09
50	0.418	4.1×10^{-5} (0.010%)	0.4179 (99.967%)	9.70×10^{-5} (0.023%)	0.418	10.62
100	0.836	1.62×10^{-4} (0.019%)	0.8357 (99.969%)	9.70×10^{-5} (0.012%)	0.836	10.92
150	1.253	3.64×10^{-4} (0.029%)	1.2525 (99.963%)	9.70×10^{-5} (0.0077%)	1.253	11.09
200	**1.671**	**6.48×10^{-4}** (0.039%)	**1.6703** (99.955%)	**9.70×10^{-5}** (0.0058%)	**1.670**	**11.22**
250	2.089	1.012×10^{-3} (0.048%)	2.0879 (99.947%)	9.70×10^{-5} (0.0046%)	2.089	11.32
300	2.507	1.457×10^{-3} (0.058%)	2.5054 (99.938%)	9.70×10^{-5} (0.0039%)	2.506	11.39
500	4.178	4.043×10^{-3} (0.097%)	4.1739 (99.901%)	9.70×10^{-5} (0.0023%)	4.174	11.62
1000	8.355	0.01614 (0.193%)	8.3388 (99.806%)	9.70×10^{-5} (0.0012%)	8.339	11.92
2000	16.711	0.06431 (0.385%)	16.6466 (99.6146%)	9.70×10^{-5} (5.8×10^{-4}%)	16.647	12.21
3000	25.066	0.1441	24.9218	9.70×10^{-4}	24.922	12.39

Table 4A. Continuation

$[SrS]_S$ $mg \cdot L^{-1}$	$[Sr^{2+}]$ mM	$[S^{2-}]$ mM, %	$[HS^-]$ mM, %	$[H_2S]_w$ mM	$[OH^-]$ mM	pH (calc.)
		(0.575%)	(99.425%)	(3.87×10^{-3}%)		
4000	33.421	0.2553	33.1656	9.70×10^{-4}	33.166	12.52
		(0.764%)	(99.236%)	(2.90×10^{-3}%)		
5000	41.776	0.3974	41.3786	9.70×10^{-4}	41.379	12.61
		(0.951%)	(99.049%)	(2.32×10^{-3}%)		
6500	54.309	0.5686	53.7394	9.70×10^{-4}	53.739	12.73
		(1.047%)	(98.951%)	(1.79×10^{-3}%)		
8500	71.019	1.0141	70.0048	9.70×10^{-4}	70.005	12.85
		(1.428%)	(98.572%)	(1.37×10^{-3}%)		
10000	83.552	1.4279	82.1241	9.70×10^{-4}	82.124	12.92
		(1.709%)	(98.291%)	(1.16×10^{-3}%)		

Table 4B. Experimentally measured values of pHs, concentrations of ions ($[Sr^{2+}]$, $[OH^-]$) and all sulphur forms (S_{total}, including $[HS^-]$) in 0.125–88.064 mM [SrS] aqueous solutions [7,9].

$[SrS]_S$ (mM) (SD ±)	pH (SD ±)	$[OH^-]$ (mM) (SD ±)	$[Sr^{2+}]$ (mM) (SD ±)	$[S_{total}]$ (mM) (SD ±)	$[HS^-]$ (mM)[b] (SD ±)
0.125±0.01	10.00±0.02	0.100	0.117±0.04	0.122±0.05	0.107±0.06
0.418±0.01	10.64±0.02	0.437	0.345±0.06	0.411±0.04	0.374±0.03
0.836±0.01	10.97±0.02	0.933	0.659±0.06	0.821±0.05	0.782±0.03
1.253±0.01	11.16±0.02	1.445	0.975±0.08	1.232±0.06	1.229±0.04
1.671±0.01	**11.18±0.02**	**1.514**	**1.356±0.08**	**1.647±0.05**	**1.643±0.03**
2.089±0.01	11.28±0.02	1.905	1.625±0.08	2.054±0.10	1.892±0.06
2.507±0.01	11.42±0.02	2.630	2.014±0.10	2.429±0.15	2.106±0.06
4.178±0.02	11.60±0.02	3.981	3.286±0.12	3.472±0.27	3.368±0.18
8.355±0.02	12.05±0.02	11.220	6.512±0.14	7.991±0.35	7.356±0.30
16.711±0.03	12.36±0.02	22.909	12.56±0.16	16.54±0.65	14.54±0.48
25.066±0.03	12.55±0.02	35.481	18.25±0.20	24.83±0.76	24.02±0.66
33.421±0.03	12.67±0.02	46.774	24.82±0.26	32.03±0.98	26.86±0.84
41.776±0.04	12.78±0.02	60.256	31.78±0.38	38.67±1.25	35.11±0.98
54.309±0.04	12.92±0.02	83.176	40.49±0.44	49.58±1.46	43.88±1.20
71.019±0.05	13.04±0.02	109.648	52.32±0.48	63.56±2.08	54.34±1.92
83.552±0.06	13.11±0.02	128.825	59.04±0.56	73.72±2.54	61.22±2.18
88.064±0.06	13.12±0.02	131.826	59.38±0.64	NA	NA

[a] Measured iodometrically
[b] Measured spectrophotometrically
NA – not applicable

The results of the measurements showed (Tables 3, 4A and 4B) that the final pH's of the closed equilibrium systems of CaS–H_2O or SrS–H_2O depended on the amount of added CaS or SrS salt into purified (MilliQ) water. Besides, the experimental results corresponded to the theoretical model, as the calculated concentrations of formed ions, molecules and pH in CaS–H_2O or SrS–H_2O equilibrium systems (at [CaS] 0.335–1.823 mM or at [SrS] 0.125–83.552 mM) were close to the measured values, especially at lower amounts of added CaS ([CaS] ≤ 1.733 mM) or SrS ([SrS]≤1.671 mM) salt (these solutions pH's were below 11.5). Thus, the experimental data indicated that the first equilibrium state was detected at the CaS–H_2O or SrS–H_2O closed equilibrium system's pH values about 11.18±0.02, which also corresponds to saturation state of these aqueous solutions (e.g. [CaS]= 1.733±0.01 mM or [SrS]=1.671±0.01 mM) [7,8].

According to experimental results, the solubility of CaS (calculated at system's state of equilibrium) was 125.0 $mg \cdot L^{-1}$ (1.733 mM) and for SrS it was 200 $mg \cdot L^{-1}$ (1.671 mM) in these closed equilibrium systems (the corresponding system's pH values at 25 ºC were about 11.22±0.04). Therefore, the solubility of CaS at equilibrium state or equilibrium constant (K_c) was evaluated to be $2.912 \cdot 10^{-6}$ $(mol \cdot L^{-1})^2$, and for SrS, $K_{c,SrS}=2.143 \cdot 10^{-6}$ $(mol \cdot L^{-1})^2$. Recent studies have shown that the calculated values of K_{SP} for CaS–H_2O or SrS–H_2O equilibrium systems are still inaccurate, because direct determination of S^{2-} ions is technically difficult due to their rapid reaction with protons, which causes significant increase in pH values of these systems, as indicated in Figure 4 [7,8,25, 50–52].

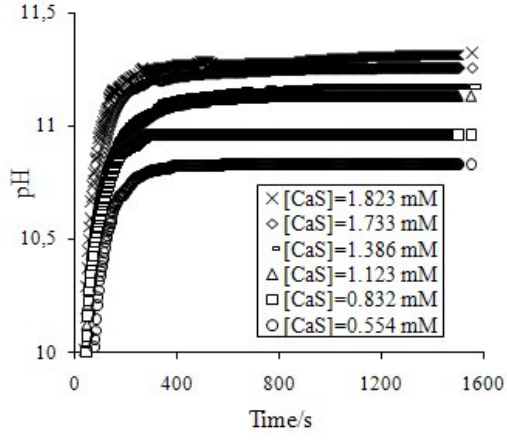

Figure 4. The obtained pH profiles and their time dependence (Time/s) during dissolution of solid CaS in water at 25 ºC [8].

As seen in Tables 3, 4A and 4B, the main species of sulphur in the CaS and SrS aqueous solutions (in the measured pH range of 10.0–13.1) was bisulphide (HS^-), which content was about 81–99% of total amount of dissolved sulphurous compounds (S_{total}). In addition, the measured values of [Ca^{2+}], [Sr^{2+}] (determined by direct titration with EDTA titration) and [OH^-] ions (potentiometrically with Jenway 3520 pH-meter) showed increase in their values at higher [CaS] or [SrS] in aqueous solutions. Besides, the pH increased further even after visual appearance of solid phase due to supersaturation (this occurs with a solution when the concentration of a solute exceeds the concentration specified by the value of solubility at equilibrium) in CaS–H_2O (Figure 5) or SrS–H_2O (Figures 6A and 6B) closed equilibrium systems. The latter can be explained by the formation of $(H_2S)_w$ in these closed equilibrium systems, which increases the solubility of CaS or SrS salt in aqueous solutions as described in earlier studies [7–9,20,24].

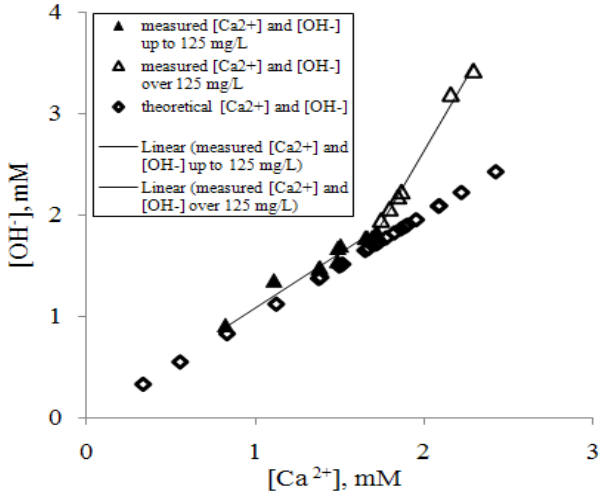

Figure 5. Relationship between concentrations of measured and theoretically calculated [Ca^{2+}] and [OH^-] at [CaS] from 0.832 to 2.424 mM [8].

Comparison of the measured [Ca^{2+}] or [Sr^{2+}] and [OH^-] (Tables 3, 4A and 4B) showed that the concentration of calcium or strontium ions were lower than [OH^-] at larger amount of added CaS or SrS salt into MilliQ water. For example, the ratio of the practically measured [Ca^{2+}] to [OH^-] had the mean value of 0.906 (±0.044) for 0.335–1.823 mM [CaS] aqueous solutions, but at [CaS]≥1.733 mM, this ratio was smaller due to supersaturation, as shown in Figure 5 (relationships between [Ca^{2+}] and [OH^-]).

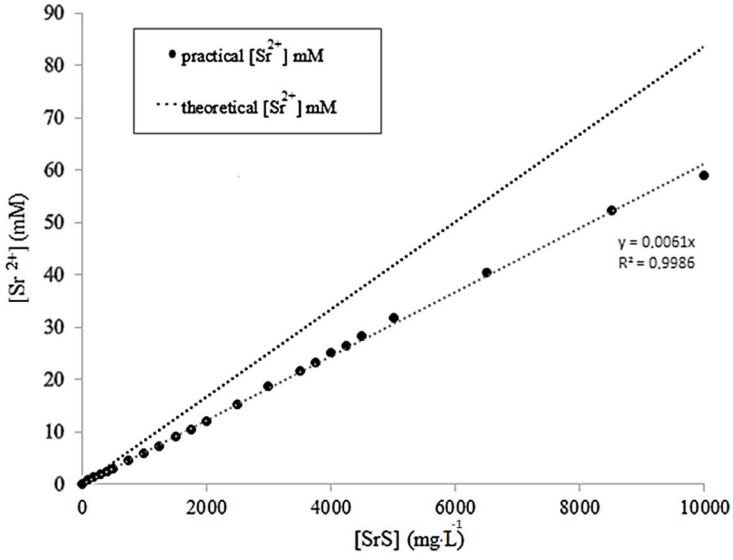

Figure 6. Calculated and measured (EDTA titration) values of $[Sr^{2+}]$ ions in SrS aqueous solutions in the range of added [SrS] 15–10000 mg·L^{-1} (0.125–83.552 mM) [7,9].

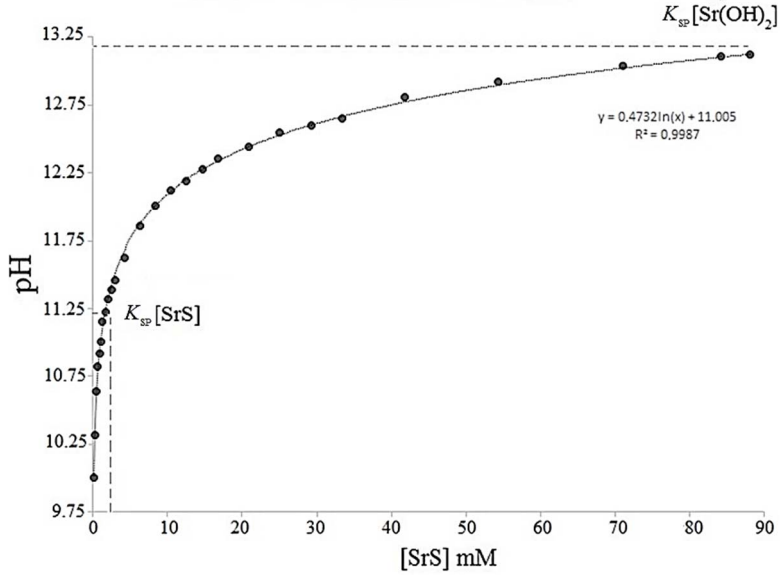

Figure 7. Measured pH values of SrS aqueous solutions (in the solid [SrS] range of 0.125–88.064 mM), where the vertical dashed line refers to the solubility point, which correspond to the values of $K_{SP,\ Sr(OH)2}$ [7,9,31].

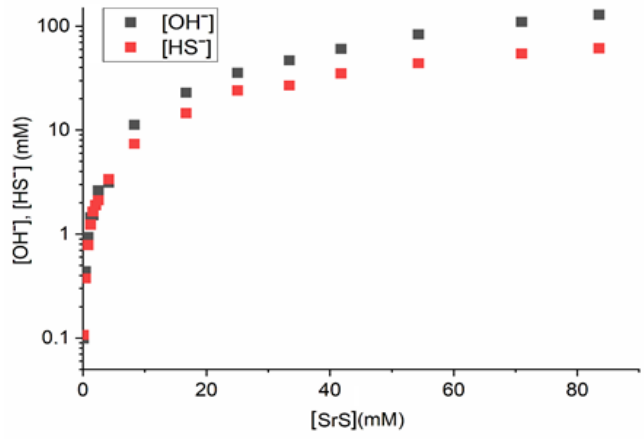

Figure 8. Correlation between the experimentally measured [HS^-] (spectrophotometrically) and [OH^-] (potentiometrically, calculated on the basis of determined pH values) ions in logarithmic scale in SrS aqueous solutions at the [SrS] range of 15–10540 mg·L^{-1} (0.125–83.552 mM) [7,9].

The measured values of [S_{total}] and the [Ca^{2+}] or [Sr^{2+}] were rather similar at lower amount of added CaS or SrS salt ([CaS]≤ 1.733 mM) or SrS ([SrS]≤1.671 mM), when supersaturation (the presence of solid phase) conditions were not present in CaS–H_2O or SrS–H_2O closed equilibrium systems (Tables 3, 4A and 4B). Moreover, the concentration of these ions in the CaS or SrS aqueous solutions were almost equal to the calculated values at [CaS]≤1.386 mM or [SrS]≤1.67 mM as the added CaS or SrS salt was dissociated completely (Figures 5 and 6). Besides, measured amounts of total sulphide species [S_{total}] in these systems (mainly in a form of HS^-), as well as [Sr^{2+}], decreased along with the increase in [CaS] or [SrS].

Additionally, the measured ratio of [S_{total}]/[OH^-] in the supersaturated CaS or SrS aqueous solutions was significantly lower (*p-value* <0.05) compared with [CaS]≤1.733 mM or [SrS]≤1.671 mM (Tables 3, 4A and 4B). According to Figures 5, 7 and 8, the obtained results of measurements indicated that [OH^-] exceeded [HS^-] in CaS–H_2O or SrS–H_2O closed equilibrium systems when supersaturation visually appeared at higher salt concentration ([CaS]≥1.733 mM or [SrS]≥1.671 mM). As seen in Figures 7 and 8, determined [OH^-] ions in the latter system remained almost unchanged at pH ≤13.1 because the solubility product (K_{SP}) value for $Sr(OH)_2$ was exceeded at [SrS]≥83.552 mM (≥10000 mg·L^{-1}) and precipitation (in the form of strontium octahydrate, $Sr(OH)_2 \cdot 8H_2O$) occurred [7,9]. Thus, the difference in their concentrations in CaS or SrS aqueous solutions is connected with the autoprotolysis of water, where a surplus number of protons ($\Delta[H^+]_{H_2O}$), will be bound by sulphide ions after the dissociation of corresponding salt. Therefore, the latter should also be taken to account in developing the given theoretical models for the CaS–H_2O or SrS–H_2O closed equilibrium systems [7–9].

Previous studies carried out by Tamm et. al (2016) also showed that the CaS–H_2O equilibrium system's pH depended on the amount of the solid phase (e.g., oil shale ash) added [13]. Thus, the greater was the amount of initial oil-shale ash (it also contains CaS and SrS), the higher was the concentration of sulphide species in the liquid phase [13,77,78]. In the closed equilibrium systems of CaS–H_2O or SrS–H_2O, the experimental results corresponded to the theoretical model, which supported the validity of the developed novel proton transfer model linking different acid–base equilibria. The same approach can be applied to complex systems involving more acid–base equilibria (e.g., the equilibrium of calcium carbonate with ammonia nitrogen or phosphoric acid). In comparison with the equilibrium system of H_2O–$(CO_2)_W$–$CaCO_3$, the liquid phase (water) was only in contact with solid phase and the volume of the gas phase was negligible [7–9, 50–52].

3.2 Results of the NTA measurements of dissolved SrS or CaS particles in deoxygenated aqueous solutions

Previous studies have indicated that by experimental measurements it is still an issue to estimate visually the precise moment, when the precipitate forms (or supersaturation occurs) in the CaS or SrS aqueous solutions, which consist of very small (0.001–1 μm of size) colloidal particles [7–9,25,62]. The latter tend to form larger particles (≥450 nm of size) as a result of their coagulation and will then become visible in colloidal systems (also known as Tyndall effect) [65,68]. Thus, the validity of particle size distributions for a sample depended on the accurate sizing of particles as well as on precise concentration measurements. As seen in Figure 9 at lower salt concentration ([CaS] or [SrS]≤0.1 mM) dissolved ions (or molecules) and their pairs were first formed after dissolution of CaS or SrS salt in aqueous media. As the smallest nanoparticles (detected by the Nano-Sight LM10 viewing unit) were in size of 10 nm or above (the lower detection limit of NTA instrument), they firstly appeared in the observed equilibrium systems at [CaS] or [SrS] less than about 0.1 mM. Besides, also disordered aggregates and crystals appeared in prepared samples (filtrated through 0.45 μm membrane filters) taken from the closed equilibrium systems of CaS–H_2O or SrS–H_2O when larger amounts of CaS or SrS salt were added (mainly due to the co-agulation of nanoparticles), and as a result, the supersaturation (precipitation of dissolved CaS or SrS salt in the form of calcium or strontium octahydrate) occurred (Figure 9) [9, 25, 62, 86, 87].

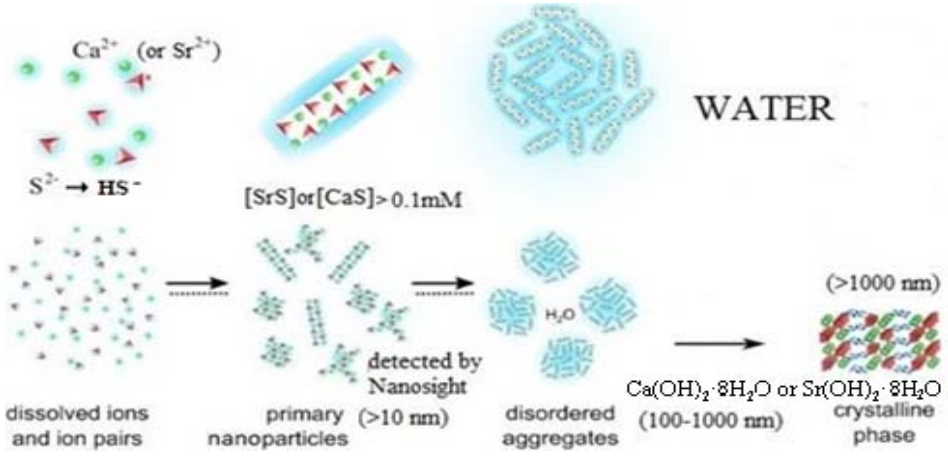

Figure 9. The comprehensive size of formed particles in the closed equilibrium systems of CaS–H_2O or SrS–H_2O depending on the added amount of salt ([$CaS_{(s)}$] or [$SrS_{(s)}$]) into an aqueous media [25,88].

However, previous studies indicated that the NTA instruments used for particles concentration measurements still have been shown low precision, due to variation in their number detected between video replicate measurements of the same sample. According to the relevant literature data, the measurement accuracy of the NTA instrument is generally within 5% of the expected particle size once correct hardware and software settings have been applied [25,82,83]. For low particle counts, it has been suggested that increasing video replicates (e.g., from 5 to 15 times) could lead to more precise concentration measurements. As seen in captured photo taken by using NTA instrument (Figure 10), it allowed the distinction of two or more light scattering centres for very large aggregates (>1 μm), which suggested that they were formed by the assembly of smaller ones. However, the brightness of such large particles interferes with the optimization of the instrument settings, it makes smaller aggregates more difficult to detect in aqueous media [25,62,83,86–90].

Figure 10. Captured image of the formed SrS particles (surrounded by a series of diffraction rings) in MilliQ water in the NTA video frame.

According to the obtained results from the CaS–H_2O or SrS–H_2O closed equilibrium systems, the first detectable particles in the analysed samples were measured by NTA instrument containing 0.097±0.01 mM of $CaS_{(s)}$ (pH=9.94±0.02) (Fig. 11) and 0.092±0.01 mM of $SrS_{(s)}$ (pH=9.97±0.02) (Fig. 12) or above these amounts of added CaS or SrS salt. This was about 18 times lower concentration than our previously determined system's equilibrium constant (K_c) or solubility values at [SrS]=1.671 mM and [CaS]=1.733 mM (pH=11.22±0.04) for given systems by using potentiometry. Its corresponding values, where nanoparticles (≤10 nm) were firstly detected by NTA, were calculated to be $K_{c,CaS}=9.409\cdot10^{-9}$ $(mol\cdot L^{-1})^2$, and $K_{c,\,SrS}=8.464\cdot10^{-9}$ $(mol\cdot L^{-1})^2$, respectively. Up to these amounts of added salt (CaS or SrS) in the closed equilibrium systems of CaS–H_2O and SrS–H_2O, all particles were dissolved in aqueous media due to the better solubility of smaller particles in the nanoscale region. Thus, no particles were detected by the NTA method below the concentrations stated above. In addition, the occurrence of NPs was related to increase in the concentration of Sr^{2+} and Ca^{2+} ions and the increase in the pH values of these equilibrium systems when an additional amount of salt (CaS or SrS) was dissolved [7–9,25,62].

As shown in Figures 11 and 12, the size distribution and the average concentration of formed particles in the closed equilibrium systems of CaS–H_2O and SrS–H_2O increased upon adding more CaS or SrS salt into deoxygenated MilliQ water (mainly due to the coagulation of smaller particles into larger ones). As a result, the overall concentration ratio of the formed particles to the amount of the added CaS or SrS salt decreased in these closed equilibrium systems [25,62].

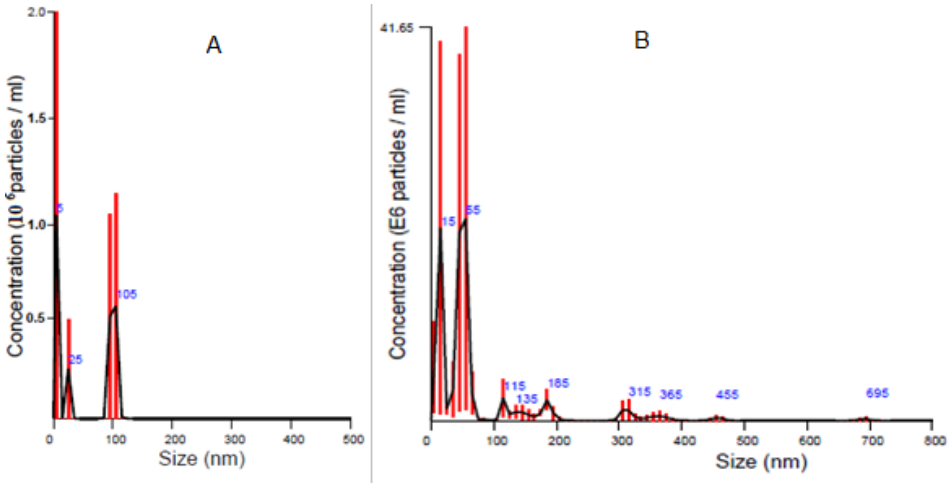

Figure 11. Size distribution (nm) and the average concentration of particles (ACP) from the NTA measurements in the closed equilibrium system of CaS–H_2O at 25±0.2 °C (red error bars indicate the standard error of ACP in this system): **A**) at [CaS]=0.097±0.01 mM (pH=9.94±0.02), ACP is 1.35±0.57·10^6 per mL; **B**) at [CaS]=1.388±0.01 mM (pH= 11.17±0.02), ACP is 9.07±3.96·10^7 per mL.

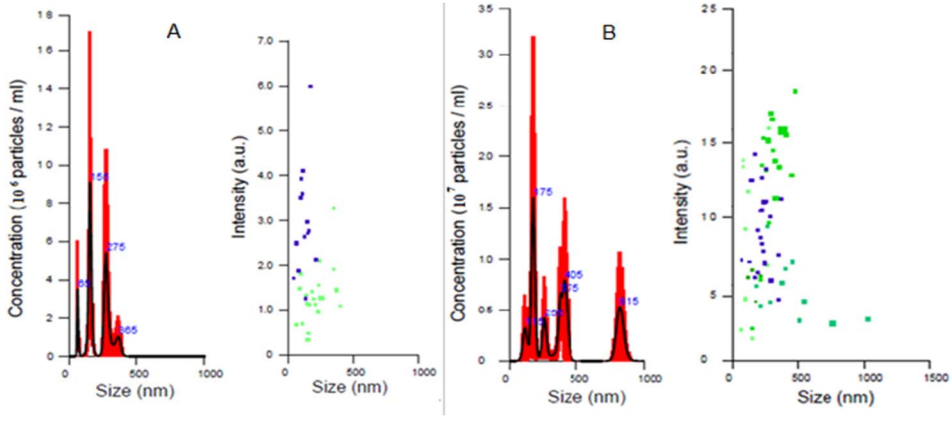

Figure 12. Size distribution (nm) and the ACP from the NTA measurements in the closed equilibrium system of SrS–H_2O at 25±0.2 °C: **A**) at [SrS]=0.092±0.01 mM (pH= 9.97± 0.02), ACP is 5.41±4.38·10^6 per mL; **B**) at [SrS]=1.671±0.01 mM (pH=11.18±0.02), ACP is 1.74±0.61·10^7 per mL.

The former studies with calcium hydroxide indicated that its nanoparticles were detected in samples starting from 0.5 g·L^{-1} (pH≥12.3) of added salt or when the $Ca(OH)_2$ aqueous solution's pH was increased approximately to the same value by the addition of NaOH, which pushed back salt dissolution, into this closed equilibrium system, as the value of $K_{SP,Ca(OH)_2}$ was exceeded [62]. Thus, this principle allows to calculate the K_{SP} or K_c value for nanoscale particles in different equilibrium systems by using a novel NTA method [25,62,79,83–85].

3.3 Results of $(H_2S)g$ bonding rate by NaOH solution in the closed equilibrium system of SrS–H_2O

The results of experimental measurements in a closed test system of SrS–H_2O indicated that the gaseous hydrogen sulphide average bonding rate by 0.5M of NaOH solution was 0.827 $\mu g \cdot h^{-1} \cdot cm^{-2}$. As shown in Table 5, $(H_2S)_g$ emission from initially prepared 4.18–16.71 mM of the SrS aqueous solution and its fixation by alkaline solution (determined by iodometric titration) also depended on added amount of salt, duration of the experiment and the size of the gas-liquid interface [7].

Ebrahimi et al. (2003) have found that the reaction between H_2S and NaOH solution at higher concentrations is instantaneous and it takes place at the gas-liquid interface [91]. Thus, at a higher salt concentration it takes a longer time to establish chemical equilibrium between dissolved sulphide and $(H_2S)_g$ ions in the CaS or SrS aqueous solutions. As the latter could additionally increase the solubility of CaS or SrS salt in the CaS–H_2O or SrS–H_2O closed equilibrium systems, it must be considered by making calculations of these systems' parameters (e.g., aqueous solubility, pH). Besides, $HS^-_{(aq)}$ will be the predominant sulphide species in most, if not all (since the problem of oxidation was understood in earlier studies), aqueous alkaline solutions [91,92].

Table 5. Experimentally measured pH, dissolved $[Sr^{2+}]$ in SrS aqueous solution and bonded $(H_2S)_g$ in the form of sulphide sulphur by alkaline (0.5 M NaOH) solution.

SrS (H_2S)						
$g \cdot L^{-1}$	mM	pH	Duration of the experiment (h)	$[Sr^{2+}]$ (mM) (dissoluted)	$[S^{2-}]_{total}$ ($mg \cdot L^{-1}$) in 0.5 M NaOH solution	$(H_2S)_g$ bonding rate into 0.5 M NaOH solution ($\mu g \cdot h^{-1} \cdot cm^{-2}$)
0.5	4.18	11.42	141	3.11(±0.10)	72.3(±3.9)	0.774
0.75	6.27	11.61	118	4.12(±0.05)	62.5(±7.8)	0.796
1	8.36	11.81	68	5.44(±0.04)	41.2(±3.9)	0.913
1.25	10.44	11.98	71	7.76(±0.12)	31.8(±7.8)	0.679
1.5	12.53	11.85	164	8.08(±0.04)	92.1(±7.8)	0.846
1.75	14.62	12.15	68	10.12(±0.04)	41.8(±7.8)	0.917
2	16.71	12.16	238	11.15(±0.02)	135.5(±7.8)	0.861
						Average = 0.827

The chemical oxidation of hydrogen sulphide proceeds through a chain reaction mechanism. In the first step, it is transformed in the presence of oxygen to elemental sulphur [93]. Finally, after multiple intermediate oxidation reactions, the polysulphide anions (e.g., $S_2O_3^{2-}$) will be formed (they are stable at pH=~7–12) [93,94]. At lower pH values the latter reacts with hydrogen sulphide, and as a result, the elemental sulphur forms again in aqueous media [93–95].

4. CONCLUSIONS

The aims of the current PhD thesis were to investigate the dissolution process of CaS or SrS in ultrapure MilliQ water and to determine these closed equilibrium system's ($CaS–H_2O$ or $SrS–H_2O$) essential parameters (e.g., pH and the K_{SP}). In addition, also to upgrade our previously developed mathematical models for the $CaS–H_2O$ or $SrS–H_2O$ closed equilibrium systems based on the proton transfer principle, which were also experimentally validated.

The goals were achieved for given closed equilibrium systems by using experimentally measured concentrations of the formed ions (Sr^{2+}, OH^-, HS^-, H_2S, S^{2-}) and describing their interactions in a structural scheme. These equilibrium system's pH values and the concentrations of sulphide species were determined potentiometrically, spectrophotometrically and by iodometric titration. The solubility of CaS was evaluated to be 1.733 mM and its value for SrS was 1.671 mM (pH= 11.22±0.04) at 25 ºC and by normal pressure. In addition, the average bonding rate of $(H_2S)_g$ by 0.5 M NaOH in a closed oxygen-free test system was experimentally measured and the obtained transformation speed value was 0.827 $\mu g \cdot h^{-1} \cdot cm^{-2}$ (**Papers I, II, V)**.

Besides, the size dependence and average concentrations of the formed particles (measured in the range of 10–1500 nm) on the amount of added CaS or SrS salt in these closed equilibrium systems were studied by using a NTA. According to NTA measurements, the first detectable particles in the analysed samples were measured by NTA instrument containing 0.097±0.01 mM of $CaS_{(s)}$ (pH=9.94± 0.02) and 0.092±0.01 mM of $SrS_{(s)}$ (pH=9.97±0.02) or above these amounts of added CaS or SrS salt. The latter was about 18 times lower than previously determined values at equilibrium state, when saturation visually occurred (particle size ≥450 nm) (**Paper VI**).

As seen from the experimental results, the solubility of CaS or SrS in MilliQ water at constant temperature also depended on pH and the concentration of the formed ions in these closed equilibrium systems, because smaller ones have better solubility. Thus, this principle allows to calculate the K_{SP} value for nanoscale particles in different closed equilibrium systems by using NTA method, which is suitable for samples taken both from monodisperse and polydisperse systems, as it has a substantially better peak resolution compared to other similar techniques intended for their characterization in liquid suspensions (**Papers I, II, V, VI**).

5. SUMMARY IN ENGLISH

The amount of generated hazardous wastes (over 90% of their total volume originates from oil-shale industry) in Estonia is largest in the world per capita. More than 80% of the oil shale is used as a solid fuel in power plants, but the remaining 20% is used for the production of shale-oil, heat and cement [96,97]. Besides, it has negative impact to the quality of environment and human health. For example, the interaction of semi-coke residue with water (as a result of complex chemical reactions) generates highly alkaline sulphur-rich leachate, a hazardous waste for the environment, which requires further processing or treatment. Besides, part of sulphur from it is emitted into the atmosphere when an ecologically toxic gaseous hydrogen sulphide (H_2S_g) forms in anaerobic conditions [3–14].

The aim of this doctoral thesis was to investigate the dissolution process of CaS or SrS in MilliQ water and to determine the important parameters (e.g., pH, water solubility or K_{SP} value, ion content) of these closed equilibrium systems ($CaS–H_2O$ or $SrS–H_2O$) using the measured ions formed in these systems (Sr^{2+}, OH^-, HS^-, H_2S, S^{2-}) concentrations and describing them as a structural scheme. In addition, the aim was to update the mathematical models previously developed by our working group for the study of these equilibrium systems. The pH values of these closed equilibrium systems and the concentrations of different forms of sulphide sulphur were determined potentiometrically, spectrophotometrically and by iodometric titration [7–9,25].

Besides, the size, distribution and average concentration of formed particles (measured in the range of 10–1500 nm) in aqueous CaS or SrS solutions at equilibrium state, which depended on the amount of added salt in these systems were investigated by using the NTA, which enables to calculate the value of the equilibrium constant (K_c) or the solubility product (K_{SP}) for nanoscale particles in different equilibrium systems [25]. The objectives also included developing non-thermodynamic mathematical models for equilibrium systems containing species of sulphurous compounds, which are taking into consideration all conjugated acid-base processes in order to calculate the pH values, concentrations of formed ions and molecules by using an iteration method [7–9,25].

Based on the experimental results, the solubility of CaS or SrS in MilliQ water at constant temperature also depended on the pH of these closed equilibrium systems and the concentration of formed ions, smaller particles being more soluble. Therefore, based on this principle, it is possible to calculate more precisely the corresponding K_{SP} value for nano-sized particles present in different closed equilibrium systems using the NTA method, which is suitable for samples taken from mono- and polydisperse systems, as its resolution is significantly better compared to other similar methods for their characterization and analysis [25].

In summary, the present thesis suggests that further investigations are needed for describing CaS and SrS solubilization in water in order to describe better their dissolution mechanism and to develop our novel proton-centric model for similar closed equilibrium systems, which can be used both to assess the effects of human activities on natural water bodies and to model industrial processes (e.g., wastewater treatment) more efficiently.

6. REFERENCES

1. Holleman, A.F., Wiberg, E., and Wiberg, N. *Inorganic Chemistry,* 1st ed. Academic Press, San Diego, 2001.
2. Patnaik, P. Handbook of inorganic chemicals. The McGraw-Hill Companies, Inc., USA, 2003, pp. 1124.
3. Reinik, J., Irha, N., Steinnes, E., Urb, G., Jefimova, J., and Piirisalu, E. Release of 22 elements from bottom and fly ash samples of oil shale fueled PF and CFB boilers by a two-cycle standard leaching test. *Fuel Process. Technol.*, 2014, 124, 147–154; doi: 10.1016/j.fuproc.2014.03.011.
4. Tillmann, D.A. *Trace Metals in Combustion Systems*. Academic Press, Enserch Environmental, Sacramento, CA, 1994.
5. Ots, A. Oil shale fuel combustion. Tallinn: Tallinn University of Technology, 2006, pp. 833.
6. Lille, Ü. Current knowledge on the origin and structure of Estonian kukersite kerogen. *Oil Shale*, 2003, 20(3), 253–263; doi: 10.3176/oil.2003.3.03.
7. Uiga, K., Tenno, T., Zekker, I., and Tenno, T. Dissolution modeling and potentiometric measurements of the SrS–H_2O–gas system at normal pressure and temperature at salt concentrations of 0.125–2.924 mM. *J. Sulfur Chem.*, 2011, 32(2), 137–149; doi: 10.1080/17415993.2011.551937.
8. Zekker, I., Tenno, T., Selberg, A., and Uiga, K. Dissolution modeling and experimental measurement of CaS-H_2O binary system. *Chin. J. Chem.*, 2011, 29(11), 2327–2336; doi: 10.1002/cjoc.201180399.
9. Uiga, K., Tenno, T., Zekker, I., Mashirin, A., and Rikmann, E. Modelling and experimental measurement of the closed equilibrium system of H_2O–SrS. *Proc. Est. Acad. Sci.*, 2020, 69(4), 287–297; doi: 10.3176/proc.2020.4.02.
10. Mõtlep, R., Kirsimäe, K., Talviste, P., Puura, E., and Jürgenson, J. Mineralogical composition of Estonian oil shale semi-coke sediments. *Oil Shale*, 2007, 24(3), 405–422; doi: 10.3176/oil.2007.3.01.
11. Mölder, L., Elenurm, A., and Tamvelius, H. Sulphur compounds in a hydraulic ash disposal system. *Proc. Est. Acad. Sci. Chem*., 1995, 44(2–3), 207–211; doi: 10.3176/chem.1995.2/3.17.
12. Harzia, H., Orupõld. K., Habicht. J., and Tenno, T. Leaching behaviour of oil shale semicoke: sulphur species. *Oil Shale,* 2007, 24(4), 583–589; doi: 10.3176/oil.2007.4.09.
13. Tamm, K., Kallaste, P., Uibu, M., Kallas, J., Velts-Jänes, O., and Kuusik, R. Leaching thermodynamics and kinetics of oil shale waste key components. *Oil Shale*, 2016, 33(1), 80–99; doi: 10.3176/oil.2016.1.07.
14. Liiv, J., Teppand, T., Rikmann, E., and Tenno, T. Novel ecosustainable peat and oil shale ash-based 3D-printable composite material. *Sustainable Mater. Technol.*, 2018, 1–7; doi: 10.1016/j.susmat.2018.e00067.
15. Rao, S.R. and Hepler, L.G. Equilibrium constants and thermodynamics of ionization of aqueous hydrogen sulfide. *Hydrometallurgy*, 1977, 2(3), 293–299; doi: 10.1016/0304-386X(77)90009-3.
16. Tsonopoulos, C., Coulson, D.M., and Inman, L.B. Ionization constants of water pollutants. *J. of Chem. and Eng. Data*, 1976, 21(2), 190–193; doi: 10.1021/je60069a008.

17. Su, Y.S., Cheng, K.L., and Jean, Y.C. Amplified potentiometric determination of $pK_{(00)}$, $pK_{(0)}$, $pK_{(1)}$, and $pK_{(2)}$ of hydrogen sulfides with Ag_2S ISE. *Talanta*, 1997, 44(10), 1757–1763; doi: 10.1016/S0039-9140(97)00045-3.
18. Sun, W., Nei, S., Young, D., and Woollam, R.C. Equilibrium Expressions Related to the Solubility of the Sour Corrosion Product Mackinawite. *Industrial and Engineering Chem. Res.*, 2008, 47(5), 1738–1742; doi: 10.1021/ie070750i.
19. Licht, S., Forouzan, F., and Longo, K. Differential densometric analysis of equilibria in highly concentrated media: determination of the aqueous second acid dissociation constant of H_2S. *Anal. Chem*., 1990, 62(13), 1356–1360; doi: 10.1021/ac00212a027.
20. Migdisov, A.A., William-Jones, A.E., Lakshtanov, L.Z., and Alekhin, Y.V. Estimates of the second dissociation constant of H_2S from the surface sulfidation of crystalline sulfur. *Geochimica et Cosmochimica Acta*, 2002, 66(10), 1713–1725; doi: 10.1016/S0016-7037(01)00896-1.
21. Licht, S. and Davis, J. Disproportionation of aqueous sulfur and sulfide: kinetics of polysulfide decomposition. *J. Phys. Chem. B*, 1997, 101(14), 2540–2545; doi: 10.1021/jp962661h.
22. López-Valdivieso, A., Robledo-Cabrera, A., and Uribe-Salas, A. Flotation of celestite with the anionic collector sodium dodecyl sulfate. Effect of carbonate ions. *Int. J. Miner. Processing*, 2000, 60(2), 79–90; doi: 10.1016/s0301-7516(00)00004-1.
23. García-Calzada, M., Marbán, M.G., and Fuertes, A.B. Stability and oxidative stabilisation of sulphided calcareous sorbents from entrained flow gasifiers. *Chem. Eng. Sci*., 2000, 55(18), 3697–3714; doi: 10.1016/S0009-2509(00)00024-5.
24. Terres, E. and Brückner, K. The system $Sr(OH)_2$–$Sr(SH)_2$–H_2O. *Z. Elektrochem*., 1920, 26, 25–32.
25. Uiga, K., Rikmann, E., Zekker, I., and Tenno, T. Detection and dissolution of sparingly soluble SrS and CaS particles in aqueous media depending on their size distribution. *Proc. Est. Acad. Sci.*, 2020, 69(4), 323–330; doi: 10.3176/proc.2020.4.07.
26. Wu, S., Uddin, A. M., Nagamine, and S., Sasaoka, E. Role of water vapor in oxidative decomposition of calcium sulfide. *Fuel*, 2004, 83, 671–677; doi: 10.1016/j.fuel.2003.10.027.
27. Lide, D.R. CRC Handbook of Chemistry and Physics, 87th Edition. CRC Press, Boca Raton, FL, 2006, pp. 2608.
28. Riesenfeld, E.H., Feld, H. Die Löslichkeit von Calciumsulfid bei Gegenwart von Schwefelwasserstoff. *Z. Anorg. Allg. Chem.*, 1921, 116(1), 213–227; doi: 10.1002/zaac.19211160121.
29. Licht, S. Aqueous solubilities, solubility products and standard oxidation-reduction potentials of the metal sulfides. *J. Electrochem. Soc.*, 1988, 135(12), 2971–2975; doi: 10.1149/1.2095471.
30. Linke, W.F. Solubilities, inorganic and metal organic compounds, K–Z. Vol. 2 (4th ed.), American Chemical Society, Washington, DC, USA, 1965, pp. 1514–1515.
31. Zumdahl, S.S. Chemistry Instructors Annotated Edition, 4nd ed. Houghton Mifflin Co., New York City, 1997.
32. Douglas, B.E., McDaniel, D.H., and Alexander J.J. Concepts and models of inorganic chemistry. 2nd ed. John Wiley and Sons, Inc., New York, 1983, pp. 234.
33. Myers, R.J. The new low value for the second dissociation constant for H_2S. *J. Chem. Educ.*, 1967, 63, 687–690.
34. Licht, S. and Manassen, J. The second dissociation constant of H_2S. *J. Electrochem. Soc.*, 1987, 134, 918–921; doi: 10.1149/1.2100595.

35. Ellis, A.J., Giggenbach, W. Hydrogen sulfide ionization and sulfur hydrolysis in high temperature solution. *Geochim. Cosmochim. Acta*, 1971, 35, 247–260; doi: 10.1016/0016-7037(71)90036-6.
36. Meyer, B., Ward, K., Koshlap, K., and Peter, L. (1983) Second dissolution constant of hydrogen sulfide. *Inorg. Chem.,* 22, 2345–2346; doi: 10.1021/ic00158a027.
37. Dickson, F.W. Solubilities of metallic sulphides and quartz in hydrothermal sulphide solutions. *Bulletin of Volcanology*, 1966, 24, 605; doi: 10.1007/bf02597181.
38. Roberts, B.E. and Tremaine, P. Vapour liquid equilibrium calculations for dilute aqueous solutions of CO_2, H_2S, NH_3 and NaOH to 300 °C. *Can. J. Chem. Eng*., 1985, 63, 294–300; doi: 10.1002/cjce.5450630215
39. Knox, J. Zur Kenntnis der ionengbildung des schwefels und der komplexionen des quecksilber. *Z. Elektrochem.*, 1906, 12, 477–481; doi: 10.1002/bbpc.19060122802.
40. Eckert, W., Electrochemical identification of the hydrogen sulphide system using a pH_2S (glass/Ag^o, Ag_2S) electrode. *J. Electrochem. Soc*., 1998, 145, 77–79.
41. Muhammad, S.S. and Sundarahm, E.V. The spectrophotometric determination of the dissociation constants of hydrogen sulfide. *J. Aci. Ind. Res.* 1961, sect. B 20, 16–18.
42. Maronny, G. Constants de dissociation de I'hydrogene sulfure. *Electrochim. Acta*, 1959, 1, 58–69; doi: 10.1016/0013-4686(59)80009-8.
43. Zavodnov, S.S. and Kryukov, P.A. The value of the second dissociation constant of hydrogen sulphide. Translated from *Izvestiya Akademii Nauk SSSR. Otdelenie Khimicheskikh Nauk*, 1960, 9, 1704–1706 (english translation: 1583–1585); doi: 10.1007/bf00909835.
44. Piché, S. and Larachi, F. Dynamics of pH on the oxidation of HS^- with iron (III) chelates in anoxic conditions. *Chem.l Eng. Sci*., 2006, 61(23), 7673–7683; doi: 10.1016/j.ces.2006.09.004.
45. Plennevaux, C., Ferrando, N., Kittel, J., Frégonèse, M., Normand, B., Cassagne, T., Ropital, F., and Bonis, M. pH prediction in concentrated aqueous solutions under high pressure of acid gases and high temperature. *Corros. Sci*., 2013, 73, 143–149; doi: 10.1016/j.corsci.2013.04.002.
46. Davison, W.A. Critical comparison of the measured solubilities of ferrous sulphide in natural waters. *Geochimica et Cosmochimica Acta*, 1980, 44, 803– 808; doi: 10.1016/0016-7037(80)90261-6.
47. Morse, J.W., Millero, F.J., Cornwell, J.C., and Richard, D. The chemistry of the hydrogen sulphide and iron sulphide systems in natural waters. *Earth Sci. Rev.*, 1987, 24, 1–42; doi: 10.1016/0012-8252(87)90046-8.
48. Zumdahl, S.S. Chemical Principles, 2nd ed. D. C. Heath and Company, Lexington, MA, 1995.
49. Mullin, J.W. Crystallization, 4th ed. Elsevier Butterworth-Heinemann, Oxford. pp. 600, 2001 (ISBN: 9780750648332).
50. Tenno, T., Rikmann, E., Zekker, I., Tenno, T., Daija, L., and Mashirin, A. Modeling equilibrium distribution of carbonaceous ions and molecules in a heterogeneous system of $CaCO_3$–water–gas. *Proc. Estonian Acad. Sci.*, 2016, 65(1), 68–77; doi: 10.3176/proc.2016.1.07.
51. Tenno, T., Uiga, K., Mashirin, A., Zekker, I., and Rikmann, E. Modeling closed equilibrium systems of H_2O–dissolved CO_2–solid $CaCO_3$. *J. Phys. Chem. A*, 2017, 121(16), 3094–3100; doi: 10.1021/acs.jpca.7b00237.

52. Tenno, T., Uiga, K., Mashirin, A., Zekker, I., Rikmann, E., and Tenno, T. A novel proton transfer model of the closed equilibrium system $H_2O–CO_2–CaCO_3–NH_X$. *Proc. Estonian Acad. Sci.*, 2018, 67(3), 260–270; doi: 10.3176/proc.2018.3.04.
53. Khodakovskii, I.L., Zhogina, V.V., and Ryzenko, B.N. Dissociation constants of hydrosulphuric acid at elevated temperatures. *Geokhimia*, 1965, 7, 827–833.
54. Skoog D.A., West, D.M., and Holler, F. J. Fundamentals of Analytical Chemistry, 6th ed. Saunders College Pub., Philadelphia, PA, 1992.
55. Skoog D.A., West, D.M., and Holler, F.J. Fundamentals of Analytical Chemistry 7th ed. Fort Worth: Saunders College Pub., Philadelphia, PA, 870 pp, 1996.
56. Kelley, C.T. Iterative Methods for Linear and Nonlinear Equations. Society for Industrial and Applied Mathematics, Philadelphia, PA, 1995; https://archive.siam.org/books/textbooks/fr16_book.pdf.
57. Khan, Ib., Saeed, K., and Khan, Id., Nanoparticles: Properties, applications and toxicities. *Arabian J. of Chemistry*, 2019, 12, 908–931; doi: 10.1016/j.arabjc.2017.05.0111878-5352Ó2017.
58. Smet, P.F., Moreels, I., Hens, Z., and Poelman, D. Luminescence in Sulfides: A Rich History and a Bright Future. *Materials*, 2010, 3, 2834–2883; doi: 10.3390/ma3042834.
59. Wang, J., Zhu, Y., Grimes, C.A., and Cai, Q. Multicolor lanthanide-doped CaS and SrS near-infrared stimulated luminescence nanoparticles with bright emission: application to broad-spectrum lighting, information coding, and bio-imaging. *Nanoscale*, 2019, 11(26), 12497–12501; doi: 10.1039/C9NR03421H.
60. Wu, S.Y.-H., Yang, K.-C., Tseng, C.-L., Chen, J.-C., and Lin, F.-H. Silica-modified Fe-doped calcium sulfide nanoparticles for in vitro and in vivo cancer hyperthermia. *J. of Nanoparticle Research*, 2011, 13, 1139–1149.
61. Wu, W., and Nancollas, G.H. A new understanding of the relationship between solubility and particle size. *J. Solution Chem*., 1998, 27(6), 521–531; doi:10.1023/a:1022678505433.
62. Tenno T., Rikmann, E., Zekker, I., and Tenno T. Modelling the solubility of sparingly soluble compounds depending on their particles size. *Proc. Estonian Acad. Sci*., 2018, 67(3), 300–302; doi: 10.3176/proc.2018.3.10.
63. Misraab, S.K., Dybowska, A., Berhanu, D., Luoma, S.N., and Valsami-Jones, E. The complexity of nanoparticle dissolution and its importance in nanotoxicological studies. *Science of The Total Environment*, 438, 225–232; doi: 10.1016/j.scitotenv.2012.08.066.
64. Reidy, B., Haase, A., Luch, A., Dawson, K.A., and Lynch, I. Mechanisms of Silver Nanoparticle Release, Transformation and Toxicity: A Critical Review of Current Knowledge and Recommendations for Future Studies and Applications. *Materials*, 2013, 6, 2295–2350; doi: 10.3390/ma6062295.
65. Young, R. O. Colloids and Colloidal Systems in Human Health and Nutrition. *Int. J. Complement Alt. Med.*, 2016, 3(6), 1–8; doi: 10.15406/ijcam.2016.03.00095.
66. Luz, E.P.C.G., Borges, M.F., Rosa, F.K.A.M.F., Infantes-Molina, A., Rodriguez-Castellon, E., and Vieira, R.S. Strontium delivery systems based on bacterial cellulose and hydroxyapatite for guided bone regeneration. *Cellulose*, 2018, 25, 6661–6679; doi: 10.1007/s10570-018-2008-8.
67. Carr, B. and Wright, M. Nanoparticle Tracking Analysis: A review of the first 1000 reports of applications and usage of NTA. Malvern Instruments Ltd, 2014; https://biotech.ufl.edu/wp-content/uploads/2019/08/NTA-bookII_Mar2015-PUBLICATION-BOOK.pdf.

68. Hiemenz, P.C. and Rajagopalan, R. Principles of colloid and surface chemistry. 3rd ed. Marcel Dekker, Inc., New York, pp. 263, 1997.
69. Sennett, P. and Olivier, J. P. Colloidal Dispersions, Electrokinetic Effects, And The Concept Of Zeta Potential. *Ind. Eng. Chem*. 1965, 57(8), 32–50; doi: 10.1021/ie50668a007.
70. Chizhik, V., Egorov, A., Pavlova, M.S., Egorova, and M., Donets, A. Structure of hydration shell of calcium cation by NMR relaxation, Car-Parrinello molecular dynamics and quantum-chemical calculations. *J. Mol. Liq*., 2016, 224, 730–736; doi: 10.1016/j.molliq.2016.10.035.
71. Greenberg, A.E., Trussell, R.R., and Clesceri, L.S. (eds). Standard methods for the examination of water and wastewater, 16th ed. American Public Health Association, Washington, D.C., 1985.
72. Pawlak, Z. and Pawlak, A.S. Modification of iodometric determination of total and reactive sulfide in environmental samples. Talanta, 1999, 48(2), 347–353; doi: 10.1016/s0039-9140(98)00253-7.
73. Koh, T. and Okabe, K. Spectrophotometric determination of sulfide, sulfite, thiosulfate, trithionate and tetrathionate in mixtures. Analyst, 1994, 119(11), 2457–2461; doi:10.1039/an9941902457.
74. Thomas, O. and Burgess, C. UV-visible spectrophotometry of water and wastewater, Volume 27, 1st ed. Elsevier Science, 2007.
75. Rickard, D. and Luther, G.W. Metal sulfide complexes and clusters. *Rev. Mineral. Geochem*., 2006, 61(1), 421–504; doi:10.2138/rmg.2006.61.8.
76. Pouly, F., Touraud, E., Buisson, J.-F., and Thomas, O. An alternative method for the measurement of mineral sulphide in wastewater. Talanta, 1999, 50, 737–742; doi: 10.1016/s0039-9140(99)00201-5.
77. Tamm, K., Uibu, M., Kallas, J., Kallaste, P., Velts-Jänes, O., and Kuusik, R., Thermodynamic and kinetic study of CaS in aqueous systems. *Fuel Processing Techn.*, 2016, 142, 242–249; doi: 10.1016/j.fuproc.2015.10.029.
78. Tamm, K., Kallas, J., Kuusik, R., and Uibu, M. Modelling continuous process for precipitated calcium carbonate production from oil shale ash. Energy Procedia, 2017, 114, 5409–5416; doi: 10.1016/j.egypro.2017.03.1685.
79. Wright, M. Nanoparticle Tracking Analysis for the Multiparameter Characterization and Counting of Nanoparticle Suspensions, in Nanoparticles in Biology and Medicine. *Methods in Molecular Biology*, 2012, 906, 511–524; doi: 10.1007/978-1-61779-953-2_41.
80. Maguire, C.M., Rösslein, M., Wick, P., and Prina-Mello, A. Characterisation of particles in solution – a perspective on light scattering and comparative Technologies. *Sci. and Tech. of Adv. Materials*, 2018, 19(1), 732–745; doi:10.1080/14686996.2018.1517587.
81. Hole, P., Sillence, K., Hannell, C., Maguire, C., Roesslein, M., Suarez, G., Capracotta, S., Magdolenova, Z., Horev-Azaria, L., Dybowska, A., Cooke, L., Haase, A., Contal, S., Manø, S., Vennemann, A., Sauvain, J.-J., Staunton, K., Anguissola, S., Luch, A., Dusinska, M., Korenstein, R., Gutleb, A., Wiemann, M., Prina-Mello, A., Riediker, M., and Wick, P. Interlaboratory Comparison of Size Measurements on Nanoparticles Using Nanoparticle Tracking Analysis (NTA). *J. Nanopart. Res.*, 2013, 15(12), 1–12; doi: 10.1007/s11051-013-2101-8.

82. Gardiner, C., Ferreira, Y.J., Dragovic, R.A., Christopher Redman, C.W.G., and Sargent, I.L. Extracellular vesicle sizing and enumeration by nanoparticle tracking analysis. *J. of Extracellular Vesicles*, 2013, 2(19671), 1–11; doi: 10.3402/jev.v2i0.19671.
83. Filipe, V. and Hawe, A., Jiskoot, W. Critical Evaluation of Nanoparticle Tracking Analysis (NTA) by NanoSight for the Measurement of Nanoparticles and Protein Aggregates. *Pharmaceutical Research*, 2010, 27(5), 796–810; doi: 10.1007/s11095-010-0073-2.
84. Steinhauser, M.O. and Hiermaier, S.A Review of Computational Methods in Materials Science: Examples from Shock-Wave and Polymer Physics. *Int. J. of Molecular Sci.*, 2009, 10(12), 5135–5216; doi: 10.3390/ijms10125135.
85. Mourdikoudis, S., Pallares, R.M., and Thanh, N.T.K. Characterization techniques for nanoparticles: comparison and complementarity upon studying nanoparticle properties. *Nanoscale*, 2018, 10, 12871–12934; doi: 10.1039/c8nr02278j.
86. Du, S., Kendall, K., Morris, S., and Sweet, C. Measuring number-concentrations of nanoparticles and viruses in liquids on-line. *J. Chem. Technol. Biotechnol.*, 2010, 85(9), 1223–1228; doi: 10.1002/jctb.2421.
87. Röding, M., Zagato, E., Remaut, K., and Braeckmans, K. Approximate Bayesian computation for estimating number concentrations of monodisperse nanoparticles in suspension by optical microscopy. *Phys. Rev. E*, 2016, 93(6):063311; doi: 10.1103/PhysRevE.93.063311.
88. Van Driessche, A.E.S., Stawski, T.M., Benning, L.G., and Kellermeier, M. Calcium Sulfate Precipitation Throughout Its Phase Diagram. *New Perspectives on Mineral Nucleation and Growth*, 2016, Springer Int. Publishing, Cham, Switzerland, pp. 227–256; doi: 10.1007/978-3-319-45669-0_12.
89. Parsons, M.E.M., McParland, D., Szklanna, P.B., Guang, M.H.Z., O'Connell, K., O'Connor, H.D., McGuigan, C., Áinle, F.N., McCann, A., and Maguire, P. B. A Protocol for Improved Precision and Increased Confidence in Nanoparticle Tracking Analysis Concentration Measurements between 50 and 120 nm in Biological Fluids. *Front Cardiovasc. Med.*, 2017, 4(68); doi: 10.3389/fcvm.2017.00068.
90. Tuoriniemi, J., Johnsson, A-C. J. H., Holmberg, J.P., Gustafsson, S., Gallego-Urrea1, J.A., Olsson, E., Pettersson, J.B.C., and Hassellöv, M. Intermethod comparison of the particle size distributions of colloidal silica nanoparticles. *Sci. Technol. Adv. Mater.*, 2014, 15:035009, 1–10; doi: 10.1088/1468-6996/15/3/035009.
91. Ebrahimi, S., van Loosdrecht, M.C.M., Heijnen, J.J., and Kleerebezem, R. Kinetics of the reactive absorption of hydrogen sulfide into aqueous ferric sulfate solutions. *Chemical Engineering Science*, 2003, 58, 417–427.
92. May, P.M., Batka, D., Hefter, G., Königsberger, E., and Rowland, D. Goodbye to S^{2-} in Aqueous Solution. *Chem. Communications*, 2018, 54(16), 1980–1983; doi: 10.1039/c8cc00187a.
93. Chen, K.Y., Morris, J.C. Kinetics of oxidation of aqueous sulphide by oxygen. *Environ. Sci. Technol.*, ACS Publications, 1972, 11, 1201–1207; doi: 10.1021/es60065a008.
94. Giggenbach, W. Optical spectra and equilibrium distribution of polysulfide ions in aqueous solution at 20 °C. *Inorg. Chem.,* ACS Publications, 1972, 11, 1201–1207; doi: 10.1021/ic50112a009.

95. Kamyshny, A., Goifman, A., Gun, J., Rizkov, D., Lev, O. Equilibrium distribution of polysulfide ions in aqueous solutions at 25 degrees C: a new approach for the study of polysulfides' equilibria. *Environ. Sci. Technol.*, 2004, 38(24), 6633–6644; doi: 10.1021/es049514e.
96. Raukas, A., Punning, J.-M. Environmental problems in the Estonian oil shale industry. *Energy Environ. Sci.*, 2009, 2, 723–728; doi: 10.1039/B819315K.
97. Veiderma, M. Estonian oil shale – resources and usage. *Oil Shale*, 2003. 20(3), 295–303; doi: 10.3176/oil.2003.3s.02.

7. SUMMARY IN ESTONIAN

Tasakaaluliste suletud süsteemide CaS-H_2O või SrS-H_2O modelleerimine ja eksperimentaalne mõõtmine

Eestis tekkivate ohtlike jäätmete kogus (üle 90% sellest hulgast pärineb põlevkivitööstusest) on ühe elaniku kohta arvestatuna maailma riikidest suurim. Üle 80% põlevkivist kasutatakse soojuselektrijaamades tahke kütusena, kuid ülejäänud osast toodetakse põlevkiviõli, soojust ja tsementi [96,97]. Lisaks avaldab see märkimisväärselt negatiivset mõju keskkonna kvaliteedile ja ka inimeste tervisele. Näiteks poolkoksijäägi koosmõjul veega (keeruliste keemiliste reaktsioonide tulemusena) tekib väga aluseline väävlirikas nõrgvesi, keskkonnaohtlik jääde, mis vajab enne loodusesse laskmist edasist käitlemist. Pealegi paiskub osa sellest pärinevast väävlist atmosfääri, kui tekib anaeroobsetes tingimustes ökotoksiline gaasiline divesiniksulfiid (H_2S_g) [3–14].

Käesoleva doktoritöö eesmärk oli uurida CaS või SrS lahustumisprotsessi ülipuhtas MilliQ vees ja määrata nende suletud tasakaaluliste süsteemide (CaS–H_2O või SrS–H_2O) olulised parameetrid (nt pH, vesilahustuvus või K_{SP} väärtus, ioonide sisaldus), kasutades selleks antud süsteemides mõõdetud moodustunud ioonide (Sr^{2+}, OH^-, HS^-, H_2S, S^{2-}) kontsentratsioone ning kirjeldades neid kokkuvõtliku struktuurskeemina. Lisaks oli eesmärgiks uuendada meie töörühma poolt varasemalt välja töötatud matemaatilisi mudeleid antud tasakaaluliste süsteemide uurimiseks, mis põhinesid prootonite ülekandmise põhimõtetel, mida ka eksperimentaalselt tõestati. Nende suletud tasakaaluliste süsteemide pH-väärtused ja erinevate sulfiidse väävli esinemisvormide kontsentratsioonid määrati potentsiomeetriliselt, spektrofotomeetriliselt ja jodomeetrilise tiitrimisega. Eksperimentaalsete tulemuste põhjal arvutati CaS vesilahustuvuseks suletud süsteemi tasakaaluolekus (25 ºC konstantsel temperatuuril ja normaalrõhul) 125 $mg \cdot L^{-1}$ (1.733 mM) ning SrS puhul oli vastavaks väärtuseks 200 $mg \cdot L^{-1}$ (1.671 mM) (pH=11.22±0.04), millele vastavaks lahustuvuse või tasakaalukonstandi (K_C) väärtusteks antud tasakaaluliste süsteemide puhul saadi arvutuslikult: $K_{C,CaS}$= $2.912 \cdot 10^{-6}$ $(mol \cdot L^{-1})^2$; $K_{C,SrS}$=$2.143 \cdot 10^{-6}$ $(mol \cdot L^{-1})^2$ [7,8]. Samuti mõõdeti eksperimentaalselt gaasilise vesiniksulfiidi ($(H_2S)_g$) keskmist sidumiskiirust 0,5 M naatriumhüdroksiidi vesilahusega SrS–H_2O suletud hapnikuvabas testimissüsteemis ja saadi selle keskmiseks sidumiskiiruse väärtuseks 0,827 $\mu g \cdot h^{-1} \cdot cm^{-2}$ (**Papers I, II, V**).

Lisaks uuriti nanoosakeste jälgimise- ja analüüsisüsteemi (NTA) abil CaS või SrS vesilahuses moodustunud osakeste suurust ja keskmist sisaldust (määramisvahemikus 10–1500 nm) sõltuvalt antud suletud tasakaalulistesse süsteemidesse lisatud soola kogusest. Vastavalt NTA instrumendi poolt mõõdetud tulemustele tuvastati analüüsitud proovides esimesed nanoosakesed CaS vesilahuses kontsentratsioonil alates 0,097±0,01 mM (pH=9,94±0,02) ja SrS vesilahuses vastavalt 0,092±0,01 mM (pH=9,97±0,02), mis oli umbes 18 korda madalam võrreldes visuaalselt nähtavate (≥450 nm) osakeste küllastuskontsentratsiooniga antud

suletud süsteemide tasakaaluolekus, mille põhjal oli varasemates uurimustes arvutatud K_{SP} väärtused. Lähtudes katsetulemustest, sõltus CaS või SrS lahustuvus MilliQ vees konstantsel temperatuuril ka nende suletud tasakaaluliste süsteemide pH-st ja moodustunud ioonide kontsentratsioonist, väiksemad osakesed lahustuvad paremini. Seega on võimalik antud printsiibist lähtudes arvutada erinevates suletud tasakaalulistes süsteemides esinevate nanomõõtmetega osakeste jaoks vastav K_{SP} väärtus kasutades selleks nanoosakeste loendamise meetodit, mis sobib nii mono- kui ka polüdisperssetest süsteemidest võetud proovide jaoks, kuna selle lahutusvõime on oluliselt parem võrreldes teiste sarnaste meetoditega nende iseloomustamiseks ja analüüsimiseks [25].

Kokkuvõtteks on vaja teha täiendavaid uuringuid CaS ja SrS lahustumismehhanismi kirjeldamiseks vees lähtudes uuest prootonikesksest mudelist sarnaste suletud tasakaalu süsteemide jaoks, mida saab kasutada nii inimtegevusest tulenevate mõjude hindamiseks looduslikele veekogudele kui ka tööstuslike protsesside (s.h. reoveepuhastuse) modelleerimiseks.

8. ACKNOWLEDGEMENTS

First of all, I am exceptionally grateful to my first supervisor, prof. Toomas Tenno (*In memoriam*) for his hard work, persistence and optimism in motivating me to go on with the studies with optimism and patience with supervising my PhD studies during the fifteen-year period.

My greatest respect and gratitude also belong to my current supervisors, research fellows Ergo Rikmann (PhD) and Ivar Zekker (PhD), and to good colleagues Anne Paaver, and Alexey Mashirin (*In memoriam*), who helped me with measurements in laboratory, data collection, analyses and presentation (by making graphs in MS Excel, Origin, iterSrS.bas), editing and theoretical calculations for the publications used in the current PhD thesis. My sincere gratitude belongs to my colleagues from the department for their continuing support and tolerance. I am grateful to my family for their support during all the years of my PhD studies.

As regards the financial part, the PhD study was supported by the European Commission INTERREG research funding ("Improving quality of BSR waters by advanced treatment processes") and the following Estonian target-financed (SLTKT16012 and IUT20-16) research projects of the Estonian Ministry of Education and Research (No: SF0180135s08). "Processes in macro- and micro-heterogeneous and nanoscale systems and related technological applications". Also, CELSA project: "In-situ catalytic bioconversion of pharmaceutically active compounds in wastewater"); University of Tartu Development fund project: "Isolation of fungal strains (incl. molds) and cultivation in a geological fabric under laboratory conditions for the recovery of heavy metals from the sewage sludge"; "Sewage sludge treatment from heavy metals, emerging pollutants and recovery of metals by fungi (Number: 17431; Funder: Environmental Investment Center) and "Identifying best available technologies for decentralized wastewater treatment and resource recovery for India- SARASWATI 2.0" projects, are thanked. The publication costs of articles (**Papers IV–VI**) were partially covered by the Estonian Academy of Sciences.

Finally, I would also like to thank all the persons who have helped me during my PhD studies, but whose contribution I have forgotten to mention.

PUBLICATIONS

CURRICULUM VITAE

Name:	Kalev, Uiga
Date of birth:	November 15, 1981
Citizenship:	Estonian
Contact address:	University of Tartu, Institute of Chemistry, Ravila 14a, 50411, Tartu, Estonia
E-mail:	kuiga@msn.ee
Phone:	+372 55 824 85

Education:

2006–present	University of Tartu, Department of Physical Chemistry, PhD student (Environmental Technology).
2005–2006	University of Tartu, Department of Physical Chemistry, Master student (1 year, Environmental Technology).
2000–2005	University of Tartu, Department of Physical Chemistry, BSc in Environmental Technology,
1988–2000	Tartu Secondary School of Business

Trainings:

10/2014	Addenda OÜ (Project management; 4 hours)
02/1998	Vocational Education Center Of Tartu (Secretary-manager aid; 160 hours)

Work experience:

09/2020 – present	Gymnasium of Annelinn (teacher)
04/2018 – 12/2022	TBD Biodiscovery OÜ (a production operator; job description: preparation of pharmaceuticals)
03/2019–12/2019	University of Tartu, Faculty of Science and Technology, Institute of Chemistry, Engineer (0,25)
04/2011 – 04/2018	AHHAA Science Center (Guide, Project consultant; job description: consulting of math exposition and guiding customers)
10/2014 – 06/2015	Estonian Environmental Board (Project coordinator; job description: coordination and working out of Estonian Integrated Water Management System solution with IT-partner Datel AS)

Languages:

- English (very good in written and spoken)
- German (beginner in written and spoken)
- Russian (beginner in written and spoken)

Computer skills:

Specialist level:	MS Office 2021 and earlier (Word, Excel, Powerpoint, Access etc.); Open Office, IE, Chrome, Firefox, Acrobat Reader, Outlook, Movie Maker, Skype, Windows 7/8/10/11
Advanced level:	Adobe Illustrator
Beginner:	Linux, Adobe Photoshop, SPSS, Mapinfo, Autocad, MS Project, Solidworks, Origin

Driving licence:

Category:	B (since 2013)

Research interests: environmental engineering

Published scientific articles/ Avaldatud teaduslikud publikatsioonid:

Selberg, A., Budashova, J., **Uiga, K**., Tenno, T. Biodegradation of anionic surfactants in the bioremediation of oil-polluted soil. In: Proceedings: Kalmar ECO-TECH' 05 International Conference on "Waste, to Energy, Bioremediation and Leachate Treatment" and The Second Baltic Symposium on Environmental Chemistry; Kalmar, Sweden; 28.–30. November 2005. (Toim.) Hogland, W., Broby, T. Kalmar University: 2005, 405–412.

Uiga, K., Tenno, T., Zekker, I., Tenno, T. Dissolution modeling and potentiometric measurements of the SrS-H_2O-gas system at normal pressure and temperature at salt concentrations of 0.125–2.924 mM. *J. Sulfur Chem.*, 2011 32(2), 137–149; doi: 10.1080/17415993.2011.551937.

Zekker, I., Tenno, T., Selberg, A., **Uiga, K.** Dissolution Modeling and Experimental Measurement of CaS–H_2O Binary System. *Chin. J. Chem.*, 2011, 29(11), 2327–2336; doi: 10.1002/cjoc.201180399.

Tenno, T., **Uiga, K**., Mashirin, A., Zekker, I., Rikmann, E. Modeling closed equilibrium systems of H_2O–dissolved CO_2–solid $CaCO_3$. *J. Phys. Chem. A*, 2017, 121(16), 3094–3100; doi: 10.1021/acs.jpca.7b00237.

Tenno, T., **Uiga, K**., Mashirin, A., Zekker, I., Rikmann, E., Tenno, T. A novel proton transfer model of the closed equilibrium system H_2O–CO_2–$CaCO_3$–NH_X. *Proc. Estonian Acad. Sci*., 2018, 67(3), 260–270; doi: 10.3176/proc. 2018.3.04.

Uiga, K., Tenno, T., Zekker, I., Mashirin, A., Rikmann, E. Modelling and experimental measurement of the closed equilibrium system of H_2O–SrS. *Proc. Est. Acad. Sci*., 2020, 69(4), 287–297; doi: 10.3176/proc.2020.4.02.

Uiga, K., Rikmann, E., Zekker, I., Tenno, T. Detection and dissolution of sparingly soluble SrS and CaS particles in aqueous media depending on their size distribution. *Proc. Est. Acad. Sci*., 2020, 69(4), 323–330; doi: 10.3176/ proc.2020.4.07.

ELULOOKIRJELDUS

Nimi:	Kalev Uiga
Sünniaeg:	15.11.1981
Kodakondsus:	eesti
Aadress:	Tartu Ülikool, Keemia Instituut, Kolloid- ja keskkonnatehnoloogia õppetool, Ravila 14a, 50411, Tartu, Eesti
E-post:	kuiga@msn.com

Hariduskäik:

2006–praeguseni	Tartu Ülikool, PhD, keskkonnatehnoloogia
2005–2006	Tartu Ülikool, keskkonnatehnoloogia (magistriõpingud)
2005	Tartu Ülikool, BSc, keskkonnatehnoloogia
1988–2000	Tartu kommertsgümnaasium (Hansa kool)

Keelteoskus: eesti (emakeel), inglise, saksa, vene

Töökogemus:

09/2020–praeguseni	Tartu Annelinna Gümnaasium (õpetaja)
04/2018–12/2022	TBD Biodiscovery OÜ (tootmisoperaator)
03/2019–12/2019	Tartu Ülikool, Loodus- ja täppisteaduste valdkond, keemia instituut, insener (0,25)
04/2011–04/2018	SA AHHAA Keskus (giid)
10/2014–06/2015	Keskkonnaamet (projektikoordinaator, töö sisu: Eesti veemajanduse integreeritud haldamissüsteemi projekti koordineerimine, rakenduste kava väljatöötamine)

Arvutioskus: MS Office 2019 (Word, Excel, Powerpoint, Access etc.); Open Office, IE, Chrome, Firefox, Acrobat Reader, Adobe Illustrator, Nero, Outlook, Movie Maker, Linux, Adobe Photoshop, SAP, Mapinfo, Autocad, MS Project, Solidworks, Origin, Skype, Windows 7/8/10/11

Juhtimisõigus:
Kategooria: B (alates 2013)

Peamised uurimisvaldkonnad: keskkonnatehnoloogia, heitvee puhastus

Avaldatud teaduslikud publikatsioonid:

Selberg, A., Budashova, J., **Uiga, K**., Tenno, T. Biodegradation of anionic surfactants in the bioremediation of oil-polluted soil. In: Proceedings: Kalmar ECO-TECH' 05 International Conference on "Waste, to Energy, Bioremediation and Leachate Treatment" and The Second Baltic Symposium on Environmental Chemistry; Kalmar, Sweden; 28.–30. November 2005. (Toim.) Hogland, W., Broby, T. Kalmar University: 2005, 405–412.

Uiga, K., Tenno, T., Zekker, I., Tenno, T. Dissolution modeling and potentiometric measurements of the SrS-H_2O-gas system at normal pressure and temperature at salt concentrations of 0.125–2.924 mM. *J. Sulfur Chem.*, 2011 32(2), 137–149; doi: 10.1080/17415993.2011.551937.

Zekker, I., Tenno, T., Selberg, A., **Uiga, K.** Dissolution Modeling and Experimental Measurement of CaS–H_2O Binary System. *Chin. J. Chem.*, 2011, 29(11), 2327–2336; doi: 10.1002/cjoc.201180399.

Tenno, T., **Uiga, K**., Mashirin, A., Zekker, I., Rikmann, E. Modeling closed equilibrium systems of H_2O–dissolved CO_2–solid $CaCO_3$. *J. Phys. Chem. A*, 2017, 121(16), 3094–3100; doi: 10.3176/proc.2018.3.04.

Tenno, T., **Uiga, K**., Mashirin, A., Zekker, I., Rikmann, E. Modeling closed equilibrium systems of H_2O–dissolved CO_2–solid $CaCO_3$. *J. Phys. Chem. A*, 2017, 121(16), 3094–3100; doi: 10.1021/acs.jpca.7b00237.

Tenno, T., **Uiga, K**., Mashirin, A., Zekker, I., Rikmann, E., Tenno, T. A novel proton transfer model of closed equilibrium systems of H_2O–CO_2–$CaCO_3$–NH_X. *Proc. Est. Acad. Sci*., 2018, 67(3), 260–270; doi: 10.3176/proc.2018.3.04.

Uiga, K., Tenno, T., Zekker, I., Mashirin, A., Rikmann, E. Modelling and experimental measurement of the closed equilibrium system of H_2O–SrS. *Proc. Est. Acad. Sci*., 2020, 69(4), 287–297; doi: 10.3176/proc.2020.4.02.

Uiga, K., Rikmann, E., Zekker, I., Tenno, T. Detection and dissolution of sparingly soluble SrS and CaS particles in aqueous media depending on their size distribution. *Proc. Est. Acad. Sci*., 2020, 69(4), 323–330; doi: 10.3176/proc. 2020.4.07.

DISSERTATIONES TECHNOLOGIAE CIRCUMIECTORUM UNIVERSITATIS TARTUENSIS

1. **Sille Teiter**. Emission rates of N_2O, N_2, CH_4 and CO_2 in riparian grey alder forests and subsurface flow constructed wetlands. Tartu, 2005, 134 p.
2. **Kaspar Nurk**. Relationships between microbial characteristics and environmental conditions in a horizontal subsurface flow constructed wetland for wastewater treatment. Tartu, 2005, 123 p.
3. **Märt Öövel**. Performance of wastewater treatment wetlands in Estonia. Tartu, 2006, 148 p.
   Sergei Yurchenko. Determination of some carcinogenic contaminants in food. Tartu, 2006, 143 p. Published in *Dissertation Chimicae Universitatis Tartuensis,* 51.
4. **Alar Noorvee**. The applicability of hybrid subsurface flow constructed wetland systems with re-circulation for wastewater treatment in cold climates. Tartu, 2007, 117 p.
   Ülle Jõgar. Conservation and restoration of semi-natural floodplain meadows and their rare plant species. Tartu, 2008, 99 p. Published in *Dissertation Biologicae Universitatis Tartuensis*, 139.
5. **Christina Vohla**. Phosphorus removal by various filter materials in subsurface flow constructed wetlands. Tartu, 2008, 103 p.
6. **Martin Maddison**. Dynamics of phytomass production and nutrient standing stock of cattail and its use for environment-friendly construction. Tartu, 2008, 87 p.
7. **Marika Truu**. Impact of land use on microbial communities in Estonian soils. Tartu, 2008, 126 p.
8. **Elar Põldvere**. Removal of organic material, nitrogen and phosphorus from wastewater in hybrid subsurface flow constructed wetlands. Tartu, 2009, 107 p.
9. **Margit Kõiv**. Treatment of landfill leachate and municipal wastewater in subsurface flow filters using mineralized peat and hydrated oil shale ash. Tartu, 2010, 147 p.
10. **Jaanis Juhanson**. Impact of phytoremediation and bioaugmentation on the microbial community in oil shale chemical industry solid waste. Tartu, 2010, 95 p.
    Aare Selberg. Evaluation of environmental quality in Northern Estonia by the analysis of leachate. Tartu, 2010, 117 p. Published in *Dissertation Chimicae Universitatis Tartuensis,* 99.
11. **Riho Mõtlep**. Composition and diagenesis of oil shale industrial solid wastes. Tartu, 2010, 127 p.
12. **Igor Zaytsev**. Bioaugmentation in LWA-filled horizontal subsurface flow filters for wastewater treatment: Impact of flow regime, temperature and donor system Tartu, 2010, 97 p.

13. **Siiri Velling**. Microbial BOD biosensor for wastewater analysis. Tartu, 2011, 79 p.
14. **Riina Lepik**. Biodegradability of phenolic compoundsas single and mixed substrates by activated sludge. Tartu, 2011, 153 p.
15. **Liis Marmor**. Ecology and bioindicative value of epiphytic lichens in relation to air pollution and forest continuity. Tartu, 2011, 98 p.
16. **Martin Liira**. Active filtration of phosphorus in Ca-rich hydrated oil shale ash: precipitation mechanisms and recovery. Tartu, 2012, 84 p.
17. **Kristjan Karabelnik**. Advanced design and management of hybrid constructed wetlands: environmental and water purification effects. Tartu, 2012, 128 p.
18. **Hiie Nõlvak**. Influence of qPCR workflow on target gene enumeration from environmental samples in the case of bioremediation potential estimation. Tartu, 2012, 136 p.
19. **Merlin Raud**. Study of semi-specific BOD biosensors for biosensor-array. Tartu, 2013, 103 p.
20. **Ivar Zekker**. Enrichment of anaerobic ammonium oxidizing bacteria for nitrogen removal from digester effluent and anammox process acceleration by intermediate compounds. Tartu, 2013, 142 p.
21. **Annika Uibopuu**. Communities of arbuscular mycorrhizal fungi in spruce forest ecosystem and their effect on performance of forest understorey plant species. Tartu, 2013, 104 p.
22. **Jekaterina Jefimova**. Leaching of polycyclic aromatic hydrocarbons (PAHs) and heavy metals from the oil shale processing wastes and from waste-based products. Tartu, 2015, 184 p.
23. **Teele Ligi**. Bacterial community structure and its genetic potential for nitrogen removal in the soils and sediments of a created riverine wetland complex. Tartu, 2015, 127 p.
24. **Kuno Kasak**. Greenhouse gas emissions and water treatment efficiency in subsurface flow filters using various substrates. Tartu, 2016, 128 p.
25. **Martin Ligi**. Application of close range remote sensing for monitoring aquatic environment. Tartu, 2017, 146 p.
26. **Mikk Espenberg**. Impact of management on peatland microbiome and greenhouse gas emissions. Tartu, 2017, 152 p.
27. **Jens-Konrad Preem**. Forest soil bacterial community analysis using high-throughput amplicon sequencing. Tartu, 2017, 108 p.
28. **Taavi Vaasma**. Enrichment, atmospheric dispersion and deposition of naturally occurring radionuclides from oil shale-fired power plants. Tartu, 2017, 175 p.
29. **Kristjan Oopkaup**. Microbial community and its relationship with pollutant removal in treatment wetlands. Tartu, 2018, 154 p.
30. **Ergo Rikmann**. Autotrophic nitrogen removal and relevant equilibrial processes. Tartu, 2019, 179 p.
31. **Kati Klein**. Studies and treatment of inhibitory and recalcitrant wastewater. Tartu, 2021, 168 p.

32. **Thomas Schindler**. Tree stem CH_4 and N_2O fluxes in various forest ecosystems. Tartu, 2021, 182 p.
33. **Peeter Paaver**. Development of alternative binders based on oil shale fly ash. Tartu, 2021, 130 p.
34. **Kertu Tiirik**. Antibiotic resistance in connected engineered and natural aquatic environments. Tartu, 2021, 124 p.
35. **Keit Kill**. Nutrient fluxes regulation in an in-stream constructed wetland treating polluted agricultural runoff. Tartu, 2022, 144 p.
36. **Rauno Lust**. Bioelectrochemical systems for enhanced removal of nitrate from water with a low electron donor concentration. Tartu, 2022, 145 p.
37. **Mihhail Fetissov**. Spatial decision support systems for ecosystem-based marine management. Tartu, 2022, 172 p.
38. **Mohit Masta**. Isotopologue and microbiome studies for N_2O source attribution in peat soils. Tartu, 2022, 113 p.
39. **Mirjam Uusõue**. Suspended particles dynamics and characteristics in optically complex waterbodies. Tartu, 2023, 144 p.
40. **Sharvari Sunil Gadegaonkar**. Microbial and environmental factors affecting the nitrate removal efficiency from water in bioelectrochemical systems. Tartu, 2023, 124 p.